Pharmacological Characteristics and Binding Modes of Caracurine V Analogues and Related Compounds at the Neuronal α7 Nicotinic Acetylcholine Receptor

Anders A. Jensen,*,† Darius P. Zlotos,‡ and Tommy Liljefors†

Department of Medicinal Chemistry, Faculty of Pharmaceutical Sciences, University of Copenhagen, Universitetsparken 2, DK-2100 Copenhagen, Denmark, and Pharmaceutical Institute, University of Würzburg, Am Hubland, 97074 Würzburg, Germany

Received May 17, 2007

The pharmacological properties of bisquaternary caracurine V, iso-caracurine V, and pyrazino-[1,2-*a*;4,5-*a*′]diindole analogues and of the neuromuscular blocking agents alcuronium and toxiferine I have been characterized at numerous ligand-gated ion channels. Several of the analogues are potent antagonists of the homomeric α7 nicotinic acetylcholine receptor (nAChR), displaying nanomolar binding affinities and inhibiting acetylcholine-evoked signaling through the receptor in a competitive manner. In contrast, they do not display activities at heteromeric neuronal nAChRs and only exhibit weak antagonistic activities at the related 5-HT_{3A} serotonin receptor. In a mutagenesis study, five selected analogues have been demonstrated to bind to the orthosteric site of the α7 nAChR. The binding site of the compounds overlaps with that of the standard α7 antagonist methyllycaconitine, the binding of them being centered in a cation−π interaction between the quaternary nitrogen atom of the ligand and the Trp^{149} residue in the receptor, with additional key contributions from other aromatic receptor residues such as Tyr^{188}, Tyr^{195}, and Trp^{55}.

Introduction

The neurotransmitter acetylcholine (ACh[a]) exerts its effects in the central and peripheral nervous systems through two distinct families of receptors: the muscarinic ACh receptors (mAChRs) and the nicotinic ACh receptors (nAChRs). Whereas the mAChRs are G-protein-coupled receptors, the nAChRs belong to the family of ligand-gated ion channels (LGICs), also termed the "Cys-loop receptors", which also includes receptors for serotonin, γ-aminobutyric acid (GABA), and glycine.[1−5] The nAChRs are pentameric receptor complexes, and they have been divided into the muscle-type receptors (made up of α1, β1, δ, and γ/ε subunits) and neuronal receptors made up of α2−α10 and β2−β4 subunits. The neuronal nAChRs exist as homomeric receptors composed of α7 or α9 subunits or as heteromeric receptors made up of various combinations of α2−α6 and β2−β4 subunits or of α9 and α10 subunits.[1,6] The multiple nAChR subunits form a plethora of different receptor subtypes characterized by significantly different pharmacological properties, CNS expression patterns, and physiological functions. The most abundant nAChR subtypes in the CNS are the α4β2* and the α7* receptors (the asterisks indicate the potential presence of other subunits), whereas the α3β4* subtype is the predominant subtype at ganglionic synapses.[7] The neuronal nAChRs are involved in a wide range of physiological and pathophysiological processes, and they have been proposed as potential therapeutic targets in a number of neurodegenerative and psychiatric disorders, in various forms of pain, and in nicotine addiction.[1,7−10] Because augmentation of nAChR signaling seems to hold therapeutic potential for most of these indications, the medicinal chemistry efforts in the nAChR field has predominantly been focused on the development of agonists and positive allosteric modulators of the receptors.[1,11,12] However, nAChR antagonists could also possess therapeutic prospects as analgesics, antidepressants, and smoking cessation aids.[1,13,14]

Natural product chemistry has been a great source of nAChR ligands over the years.[1,11,12] Most of the nAChR ligands developed to date have been derived from compounds from natural sources, for example, the agonists nicotine and epibatidine. Furthermore, several substances of natural origin have been shown to possess unique pharmacological profiles at the nAChRs, the numerous peptide toxins from *Conus* mollusks shown to be subtype-selective nAChR antagonists being an excellent example.[1,15] Caracurine V (Figure 1) is the main alkaloid in the stem bark of *Strychnos toxifera*. Bisquaternary analogues of caracurine V and the isomeric iso-caracurine V as well as the structurally related neuromuscular blocking agents alcuronium and toxiferine I have in previous studies been shown to be allosteric enhancers of antagonist binding at the M_2 mAChR subtype.[16] Moreover, the iso-caracurine V analogues and some of the caracurine V derivatives have been reported to possess binding affinities at the muscle-type nAChR from the electric organ of *Torpedo californica* nearly as high as those observed for alcuronium and toxiferine I.[17] Very recently, a couple of bisquaternary 6*H*,13*H*-pyrazino[1,2-*a*;4,5-*a*′]diindole analogues characterized by a completely different 3D structure regarding the relative positions of the aromatic rings than caracurine V and iso-caracurine V derivatives were found to be weak allosteric modulators of mAChRs while retaining high binding affinities to the muscle-type nAChR.[18] In a search for potent antagonists for neuronal nAChR subtypes, we have characterized the pharmacological properties of these agents at recombinant neuronal nAChRs and other LGICs. Furthermore, we have investigated the molecular basis for the antagonism displayed by these compounds at the homomeric α7 nAChR subtype in a mutagenesis study.

* To whom correspondence should be addressed. Phone: +45 3533 6491. Fax: +45 3533 6040. E-mail: aaj@farma.ku.dk.
† University of Copenhagen.
‡ University of Würzburg.

[a] Abbreviations: ACh, acetylcholine; AChBP, acetylcholine-binding protein; FMP, FLIPR membrane potential; GABA, γ-aminobutyric acid; GlyR, glycine receptor; [^{3}H]MLA, [^{3}H]methyllycaconitine; HEK293, human embryonic kidney 293; LGIC, ligand-gated ion channel; mAChR, muscarinic acetylcholine receptor; MLA, methyllycaconitine; nAChR, nicotinic acetylcholine receptor; WT, wild type; 5−HT_{3A}R, 5−HT_{3A} receptor.

10.1021/jm070574f CCC: $37.00
Published on Web 08/28/2007

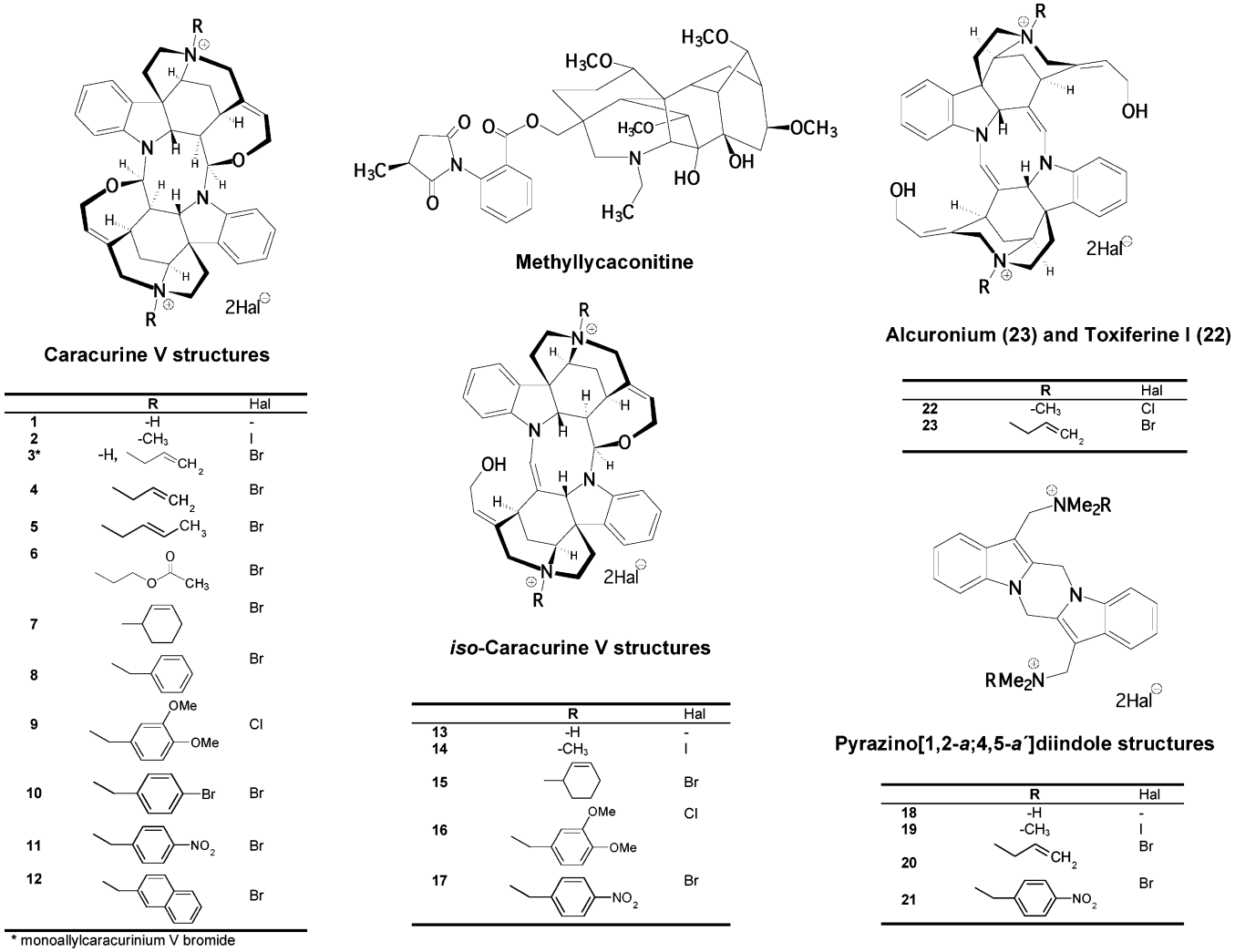

	R	Hal
1	-H	-
2	$-CH_3$	I
3*	-H, $-CH_2$	Br
4	$-CH_2$	Br
5	$-CH_3$	Br
6	$-CH_2-O-C(=O)-CH_3$	Br
7		Br
8		Br
9	2-OMe, 5-OMe	Cl
10	4-Br	Br
11	4-NO_2	Br
12		Br

	R	Hal
13	-H	-
14	$-CH_3$	I
15		Br
16	2-OMe, 5-OMe	Cl
17	4-NO_2	Br

	R	Hal
22	$-CH_3$	Cl
23	$-CH_2$	Br

	R	Hal
18	-H	-
19	$-CH_3$	I
20	$-CH_2$	Br
21	4-NO_2	Br

Figure 1. Chemical structures of compounds **1**−**23** and the reference antagonist MLA investigated in this study.

Results

Binding Properties of the Compounds to Recombinant nACh and 5-HT$_{3A}$ Receptors. The binding characteristics of the caracurine V, iso-caracurine V, and pyrazino[1,2-*a*;4,5-*a*′]-diindole analogues at human embryonic kidney 293 (HEK293) cell lines stably expressing the heteromeric rat α4*β*2, α3*β*4, and α4*β*4 nAChRs were determined in a [^{3}H]epibatidine competition binding assay. Furthermore, the compounds were characterized in a [^{3}H]methyllycaconitine ([^{3}H]MLA) binding assay to tsA-201 cells transiently transfected with an α7/5-HT$_{3A}$ chimera or with the human α7 nAChR and human Ric-3. We have previously demonstrated that the binding profiles of the α4*β*2, α3*β*4, and α4*β*4 cell lines in the [^{3}H]epibatidine binding assay are in excellent agreement with those reported for the recombinant receptors in other studies,[19−21] and the binding characteristics of the α7/5-HT$_{3A}$ chimera in the [^{3}H]MLA binding assay have been shown to be in concordance with those displayed by recombinantly expressed full-length α7 nAChRs and by native α7* receptors.[19,22,23] The caracurine V, iso-caracurine V, and pyrazino[1,2-*a*;4,5-*a*′]diindole analogues displayed binding affinities to the α7/5-HT$_{3A}$ chimera and the human α7 nAChR in the low nanomolar to low micromolar concentration ranges (Table 1). Concentration−inhibition curves for some of the analogues at the α7/5-HT$_{3A}$ chimera and the human α7 nAChR are depicted in Figures 2A and 2B. The binding affinities obtained at the chimera consisting of the amino terminal of the rat α7 nAChR and the ion channel domain of the mouse 5-HT$_{3A}$R correlated well with the affinities obtained at the human α7 nAChR (Figure 2D). In contrast, the compounds did not display significant binding to the heteromeric α4*β*2 and α4*β*4 nAChRs at concentrations up to 100 μM, and with the exception of a few analogues the compounds were not able to displace [^{3}H]epibatidine binding to the α3*β*4 nAChR in the concentrations used (Table 1).

The binding characteristics of the compounds to the human 5-HT$_{3A}$ receptor (5−HT$_{3A}$R) stably expressed in HEK293 cells were determined in a [^{3}H]GR65630 binding assay. In this assay, we obtained a K_D value of 180 pM for the radioligand, which is in agreement with other studies (data not shown).[24−26] Furthermore, the 5-HT$_3$R agonist quipazine displayed a low nanomolar K_i value, which is in concordance with a previously published binding affinity for the agonist at native 5-HT$_3$ receptors (Figure 2C).[27] The caracurine V, iso-caracurine V, and pyrazino[1,2-*a*;4,5-*a*′]diindole analogues displayed micromolar K_i values at the 5-HT$_{3A}$R (Table 1). Concentration−inhibition curves for some of the analogues at the 5-HT$_{3A}$R are depicted in Figure 2C.

Functional Characteristics of the Compounds at Five LGICs. The functional properties of the caracurine V, iso-caracurine V, and pyrazino[1,2-*a*;4,5-*a*′]diindole analogues and of the muscle relaxants alcuronium and toxiferine I at five LGICs, the α3*β*4 and α7 nAChRs, the 5-HT$_{3A}$R, the α1 glycine receptor (GlyR), and the *ρ*1 GABA$_C$R, were determined in the FLIPR membrane potential (FMP) assay (Table 2 and Figure

Table 1. Binding Characteristics of the 23 Investigated Compounds at nAChRs and 5-HT_{3A}R[a]

	r$\alpha4\beta2$-HEK293	r$\alpha3\beta4$-HEK293	r$\alpha4\beta4$-HEK293	$\alpha7/5\text{-}HT_{3A}$ (tsA-201)	hα7-hRic3 (tsA-201)	h5-HT_{3A}R-HEK293
Standard Ligands						
(*S*)-nicotine	0.0062 [8.2 ± 0.03]	0.22 [6.7 ± 0.03]	0.033 [7.5 ± 0.04]	24 [4.6 ± 0.04]	12 [5.0 ± 0.05]	nd
quipazine	nd	nd	nd	nd	nd	0.0037 [8.4 ± 0.04]
MLA	nd	nd	nd	0.0011 [9.0 ± 0.04]	0.0061 [8.2 ± 0.03]	nd
Caracurine V Analogues						
1	>100 [<4]	~30 [~4.5]	>100 [<4]	1.1 [5.9 ± 0.04]	1.1 [6.0 ± 0.00]	3.1 [5.5 ± 0.03]
2	>100 [<4]	~30 [~4.5]	>100 [<4]	0.30 [6.5 ± 0.01]	0.21 [6.7 ± 0.05]	11 [5.0 ± 0.04]
3	>100 [<4]	>100 [<4]	>100 [<4]	0.071 [7.2 ± 0.03]	0.055 [7.3 ± 0.06]	19 [4.7 ± 0.03]
4	>100 [<4]	>100 [<4]	>100 [<4]	0.066 [7.2 ± 0.05]	0.030 [7.5 ± 0.03]	~100 [~4]
5	>100 [<4]	~100 [~4]	>100 [<4]	0.23 [6.6 ± 0.05]	0.10 [7.0 ± 0.04]	15 [4.8 ± 0.04]
6	>100 [<4]	>100 [<4]	>100 [<4]	0.28 [6.6 ± 0.03]	0.31 [6.5 ± 0.05]	>100 [<4]
7	>100 [<4]	~30 [~4.5]	>100 [<4]	0.72 [6.1 ± 0.01]	0.59 [6.2 ± 0.04]	2.7 [5.6 ± 0.04]
8	>100 [<4]	>100 [<4]	>100 [<4]	0.20 [6.7 ± 0.04]	0.25 [6.6 ± 0.06]	~100 [~4]
9	>100 [<4]	>100 [<4]	>100 [<4]	0.13 [6.9 ± 0.05]	0.059 [7.2 ± 0.01]	28 [4.6 ± 0.03]
10	>100 [<4]	>100 [<4]	>100 [<4]	0.26 [6.6 ± 0.02]	0.64 [6.2 ± 0.01]	5.7 [5.2 ± 0.03]
11	>100 [<4]	>100 [<4]	>100 [<4]	0.022 [7.7 ± 0.01]	0.029 [7.5 ± 0.05]	23 [4.6 ± 0.04]
12	nd	nd	nd	0.36 [6.5 ± 0.06]	0.71 [6.2 ± 0.06]	n.d
Iso-caracurine V Analogues						
13	>100 [<4]	~30 [~4.5]	>100 [<4]	1.2 [5.9 ± 0.04]	1.7 [5.8 ± 0.01]	1.9 [5.7 ± 0.03]
14	>100 [<4]	~30 [~4.5]	>100 [<4]	0.98 [6.0 ± 0.01]	0.62 [6.2 ± 0.04]	5.9 [5.2 ± 0.06]
15	>100 [<4]	~100 [~4]	>100 [<4]	0.36 [6.5 ± 0.06]	0.23 [6.6 ± 0.04]	40 [4.4 ± 0.02]
16	>100 [<4]	>100 [<4]	>100 [<4]	0.27 [6.6 ± 0.05]	0.20 [6.7 ± 0.05]	~100 [~4]
17	>100 [<4]	>100 [<4]	>100 [<4]	0.11 [6.9 ± 0.03]	0.098 [7.0 ± 0.02]	~100 [~4]
Pyrazino[1,2-*a*;4,5-*a′*]-diindole Analogues						
18	>100 [<4]	>100 [<4]	>100 [<4]	19 [4.7 ± 0.03]	5.4 [5.3 ± 0.06]	>100 [<4]
19	>100 [<4]	>100 [<4]	>100 [<4]	2.4 [5.6 ± 0.01]	1.3 [5.9 ± 0.05]	>100 [<4]
20	>100 [<4]	>100 [<4]	>100 [<4]	4.4 [5.4 ± 0.04]	2.9 [5.5 ± 0.06]	>100 [<4]
21	>100 [<4]	>100 [<4]	>100 [<4]	2.1 [5.7 ± 0.04]	3.9 [5.4 ± 0.04]	>100 [<4]
Alcuronium and Toxiferine I						
22	>100 [<4]	~30 [~4.5]	>100 [<4]	1.6 [5.8 ± 0.03]	2.6 [5.6 ± 0.06]	>100 [<4]
23	>100 [<4]	3.2 [5.5 ± 0.03]	>100 [<4]	2.1 [5.7 ± 0.02]	1.1 [6.0 ± 0.06]	>100 [<4]

[a] The binding affinities were determined at the rat heteromeric nAChR subtypes $\alpha4\beta2$, $\alpha3\beta4$, and $\alpha4\beta4$ in a [^{3}H]epibatidine binding assay, at an $\alpha7/5\text{-}HT_{3A}$ chimera and at the human $\alpha7$ nAChR in a [^{3}H]MLA binding assay, and at the human 5-HT_{3A}R in a [^{3}H]GR65630 binding assay. The K_i values of the compounds are given in μM (with pK_i ± SEM in brackets). The data are the mean of three to nine individual experiments performed in duplicate as described in Experimental Procedures. nd: not determined.

3). The $\alpha3\beta4$-, $\alpha1$-, and $\rho1$-HEK293 cell lines have in previous studies exhibited pharmacological characteristics in the FMP assay in good agreement with those observed for the four receptors in conventional electrophysiological setups.[19,28,29] None of the investigated compounds inhibited the signaling through the two anionic LGICs, the $\alpha1$ GlyR and the $\rho1$ $GABA_CR$, at concentrations up to 100 μM (Table 2). In contrast, alcuronium, toxiferine I, and some of the caracurine V and iso-caracurine V analogues displayed weak antagonistic properties at the $\alpha3\beta4$ nAChR (Table 2). Finally, several caracurine V and iso-caracurine V analogues displayed antagonistic activities at the human 5-HT_{3A}R, and the rank order of IC_{50} values determined in the FMP assay at this receptor correlated well that of the binding affinities of the compounds in the [^{3}H]GR65630 binding assay.

Numerous studies have demonstrated that transient expression of the $\alpha7$ nAChR in mammalian cells does not result in significant cell surface expression of the receptor.[30,31] However, in recent studies coexpression of the $\alpha7$ receptor with Ric-3 has been shown to increase expression of the receptors at the cell surface.[32,33] Furthermore, the number of functional surface-expressed $\alpha7$ receptors has been shown to be under the regulation of intracellular tyrosine kinases.[34,35] Hence, in order to study $\alpha7$ nAChR function, we co-transfected human $\alpha7$ and human Ric-3 in tsA-201 cells and performed the FMP assay in the presence of genistein, a broad spectrum tyrosine kinase inhibitor. In this way we were able to obtain solid ACh-induced $\alpha7$-responses in this assay.

In the FMP assay, caracurine V itself (**1**) displayed an IC_{50} value of 1.6 μM at the $\alpha7$ nAChR, and this antagonistic potency was relatively unaltered by the introduction of N-substituents possessing different steric and electronic properties (compounds **2**−**11** in Table 2). The most pronounced changes observed were the slightly increased IC_{50} value brought on by the introduction of *p*-bromobenzyl groups as N-substituents (**10**) and the 5−6-fold lower IC_{50} values displayed by the monoquaternary and bisquaternary allyl analogues **3** and **4**, respectively, and by compound **11** bearing two *p*-nitrobenzyl groups. Interestingly, alcuronium, which is a double-ring-opening product of the diallylcaracurinium V salt **4**, displayed a 15-fold weaker antagonistic action than **4** (Table 2 and Figure 3A). The five iso-caracurine V analogues **13**−**17** displayed similar IC_{50} values at the receptor, and the pyrazino[1,2-*a*;4,5-*a′*]diindole analogues **19**−**21** were all weak antagonists at the receptor (Table 2). The rank order of the pIC_{50} values displayed by compounds **1**−**11**, **13**−**17**, **22**, and **23** at the human $\alpha7$ nAChR in the FMP assay was in reasonably good agreement with the binding affinities obtained for the compounds at the receptor (Figure 3B).

The nature of the antagonism exerted by the bisquaternary nitrobenzyl caracurinium salt **11** at the $\alpha7$ nAChR was studied in greater detail in the FMP assay (Figure 4). The presence of increasing concentrations of compound **11** or the standard competitive $\alpha7$ antagonist methyllycaconitine (MLA) resulted in right-shifted concentration−response curves for ACh characterized by significantly increased EC_{50} values and significantly decreased maximal responses for the agonist (Figure 4A). Furthermore, both antagonists exhibited higher IC_{50} values at the receptor when challenged with 100 μM ACh than with 10 μM ACh (Figure 4B).

Homology Model of the Amino-Terminal Domain of the $\alpha7$ nAChR. As can be seen from Table 1, compounds **1**−**23** exhibited similar binding affinities at the human $\alpha7$ nAChR

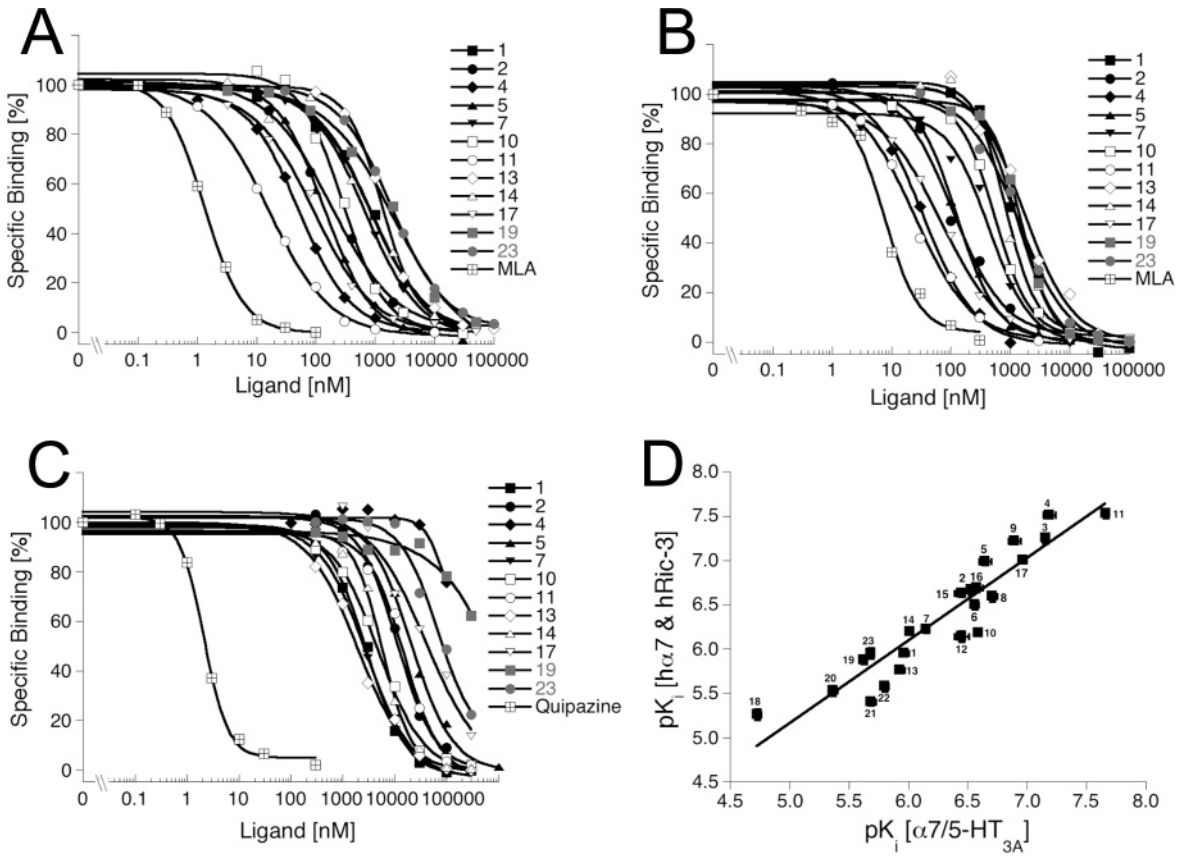

Figure 2. Binding profiles of selected compounds at the α7/5-HT_{3A} chimera in the [^{3}H]MLA binding assay (A), at the human α7 nAChR (coexpressed with human Ric-3) in the [^{3}H]MLA binding assay (B), and at the human 5-HT_{3A}R in the [^{3}H]GR65630 binding assay (C). The binding experiments were performed as described in Experimental Procedures. The figure depicts data from single representative experiments, and error bars are omitted for reasons of clarity. (D) Correlation between pK_i values obtained for compounds **1**−**23** at the α7/5-HT_{3A} and at the human α7 nAChR in the [^{3}H]MLA binding assay.

and at the α7/5-HT_{3A} chimera, whereas their binding affinities to the 5-HT_{3A}R in most cases were significantly lower. This observation strongly suggests that the compounds bind to receptor regions situated within the amino-terminal domain of the α7 nAChR. The binding mode of the ligands at the α7 nAChR was further elucidated in a mutagenesis study using a homology model of the amino-terminal domain of the α7 nAChR based on the published crystal structure of the AChbinding protein (AChBP) from *Aplysia californica* (A-AChBP) in complex with MLA.[36] Homology models of the amino-terminal domain of nAChR subtypes including α7 have previously been developed on the basis of X-ray structures of the AChBP from *Lymnaea stagnalis* (L-AChBP) in complex with various agonists.[37−40] However, these models are not suitable for studies of the binding modes of large competitive antagonists such as MLA and compounds **1**−**23**, since the crystallographic study of A-AChBP in complex with a number of agonists and antagonists have revealed a dramatic movement of the flexible C-loop (up to 11 Å) in the complexes with large antagonists including MLA compared to agonist-complexed structures.[36] This is of key importance, since the movement of the C-loop alters the positions of several residues important for ligand recognition in the A-AChBP (and in the nAChR).

The choice of the A-AChBP−MLA structure as a template for our model of the α7 nAChR binding pocket is also based on the similar sizes of MLA and caracurine V. As shown in Figure 5A, the distance between the two cationic quarternary nitrogen atoms in the caracurine V skeleton is virtually identical to the distance between the cationic nitrogen atom in MLA displaying a key cation−π interaction with Trp^{147} in its complex with A-AChBP and the distal part of the phenyl ring. The similar size of MLA and the core of the caracurine V analogues indicates that these ligands may be able to occupy a similar space in the binding pocket. The ten amino acid residues in A-AChBP situated within 4.5 Å of all four ligands in the structures by Hansen et al.,[36] six residues are identical in the α7 nAChR. This similarity increases to eight amino acids if the conservative substitutions Trp/Tyr and Ile/Leu are included.[36] Thus, the orthosteric sites of the A-AChBP and the α7 nAChR are sufficiently similar to allow us to use the structure of A-AChBP in complex with MLA and to substitute divergent residues with respect to the α7 nAChR to provide a model for the α7 nAChR binding pocket. On the basis of the observations made in the mutagenesis study described below, MLA and compound **11** were docked in the homology model, and the binding modes of the compounds are shown in Figure 5B.

Mutagenesis Study of the Binding Mode of the Compounds to the α7 nAChR. The residues identified as potential binding partners for MLA and compounds **1**−**23** were mutated to alanine residues and in some cases to other amino acid residues, and the binding properties of MLA and compounds **2**, **7**, **11**, **14**, and **19** to these mutants were determined in the [^{3}H]MLA binding assay. [^{3}H]MLA did not display significant specific binding to five of the 17 mutants (Table 3). At nine of the remaining twelve mutants, MLA and **2**, **7**, **11**, **14**, and **19** displayed binding affinities not significantly different from those at the "WT" α7/5-HT_{3A} chimera (Table 3). However, substituting the Tyr^{195} residue with an alanine residue resulted in unaltered or modestly increased K_i values for MLA, **2**, **7**, **14**, and **19** (8-, 9-, 6-, 6- and 5-fold, respectively) compared to the

Table 2. Functional Characterization of the Investigated Compounds at Five LGICs[a]

	EC_{50} [$pEC_{50} \pm$ SEM]				
	hα7 and hRic-3 (tsA-201)	rα3β4-HEK293	h5-HT_{3A}-HEK293	hρ1-HEK293	hα1-HEK293
ACh	4.0 [5.40 ± 0.02]	8.7 [5.10 ± 0.05]	nd	nd	nd
5-HT	nd	nd	0.50 [6.34 ± 0.05]	nd	nd
GABA	nd	nd	nd	0.43 [6.36 ± 0.05]	nd
Glycine	nd	nd	nd	nd	94 [4.02 ± 0.03]
	IC_{50} [$pIC_{50} \pm$ SEM]				
	hα7 and hRic-3 (tsA-201)	rα3β4-HEK293	h5-HT_{3A}-HEK293	hρ1-HEK293	hα1-HEK293
MLA	0.0083 [8.08 ± 0.03]	nd	nd	nd	nd
Caracurine V Analogues					
1	1.6 [5.80 ± 0.04]	11 [5.0 ± 0.05]	11 [4.9 ± 0.03]	>100 [<4]	>100 [<4]
2	1.5 [5.83 ± 0.06]	~30 [~4.5]	~30 [~4.5]	>100 [<4]	>100 [<4]
3	0.34 [6.47 ± 0.06]	~30 [~4.5]	~30 [~4.5]	>100 [<4]	>100 [<4]
4	0.28 [6.55 ± 0.06]	~100 [~4]	~100 [~4]	>100 [<4]	>100 [<4]
5	1.1 [5.94 ± 0.02]	~100 [~4]	~100 [~4]	>100 [<4]	>100 [<4]
6	1.6 [5.79 ± 0.05]	>100 [<4]	>100 [<4]	>100 [<4]	>100 [<4]
7	3.0 [5.52 ± 0.02]	~30 [~4.5]	4.4 [5.4 ± 0.04]	>100 [<4]	>100 [<4]
8	4.5 [5.35 ± 0.07]	>100 [<4]	~100 [~4]	>100 [<4]	>100 [<4]
9	1.3 [5.88 ± 0.04]	>100 [<4]	~30 [~4.5]	>100 [<4]	>100 [<4]
10	10 [4.98 ± 0.05]	>100 [<4]	~30 [~4.5]	>100 [<4]	>100 [<4]
11	0.37 [6.43 ± 0.05]	>100 [<4]	>100 [<4]	>100 [<4]	>100 [<4]
Iso-caracurine V Analogues					
13	1.5 [5.82 ± 0.06]	16 [4.8 ± 0.04]	2.5 [5.6 ± 0.05]	>100 [<4]	>100 [<4]
14	2.1 [5.68 ± 0.08]	~30 [~4.5]	4.2 [5.4 ± 0.02]	>100 [<4]	>100 [<4]
15	2.3 [5.63 ± 0.06]	~30 [~4.5]	~30 [~4.5]	>100 [<4]	>100 [<4]
16	2.6 [5.58 ± 0.06]	~100 [~4.5]	~30 [~4.5]	>100 [<4]	>100 [<4]
17	2.5 [5.61 ± 0.02]	>100 [<4]	~30 [~4.5]	>100 [<4]	>100 [<4]
Pyrazino[1,2-*a*;4,5-*a*′]diindole Structures					
19	30−100 [4−4.5]	>100 [<4]	>100 [<4]	>100 [<4]	>100 [<4]
20	30−100 [4−4.5]	>100 [<4]	>100 [<4]	>100 [<4]	>100 [<4]
21	30−100 [4−4.5]	>100 [<4]	~30 [~4.5]	>100 [<4]	>100 [<4]
Alcuronium and Toxiferine I					
22	9.5 [5.02 ± 0.02]	~30 [~4.5]	>100 [<4]	>100 [<4]	>100 [<4]
23	4.1 [5.39 ± 0.01]	18 [4.8 ± 0.05]	>100 [<4]	>100 [<4]	>100 [<4]

[a] The compounds were characterized functionally in the FMP assay using stable cell lines expressing the rat α3β4 nAChR, the human 5-HT_{3A}R, the human ρ1 $GABA_C$ receptor, and the human glycine α1 receptor and at tsA-201 cells transiently expressing the human α7 nAChR and human Ric-3. The EC_{50} and IC_{50} of various reference compounds and compounds **1**−**23** are given in μM with $pEC_{50} \pm$ SEM or $pIC_{50} \pm$ SEM values in brackets. For the characterization of the antagonists $EC_{70} - EC_{95}$ values of the respective agonists were used: 10 μM ACh (hα7), 20 μM ACh (rα3β4), 1 μM serotonin (h5-HT_{3A}), 1 μM GABA (hρ1), and 200 μM glycine (hα1). nd: not determined.

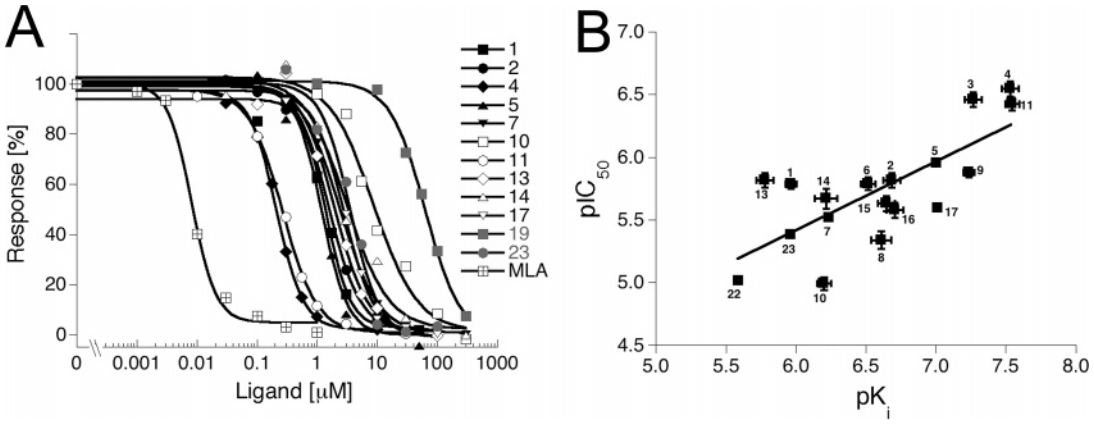

Figure 3. Functional profiles of selected compounds at the human α7 nAChR in the FMP assay. (A) Concentration−inhibition curves for MLA and compounds **1**, **2**, **4**, **5**, **7**, **10**, **11**, **13**, **14**, **17**, **19**, and **23** at the human α7 nAChR transiently coexpressed with human Ric-3 in tsA-201 cells in the FMP assay. The FMP assay was performed as described in Experimental Procedures using a final assay concentration of 10 μM ACh. The figure depicts data from a single representative experiment, and error bars are omitted for reasons of clarity. (B) Correlation between pK_i values and pIC_{50} values for compounds **1**−**11**, **13**−**17**, **22**, and **23** at human α7 nAChR coexpressed with human Ric-3 in tsA-201 cells.

"WT" chimera, whereas the binding affinity of **11** at the Y195A mutant was reduced 41-fold (Table 3). Furthermore, MLA and **11** displayed 15- and 7-fold reduced binding affinities to the W55A mutant, respectively, whereas the other four compounds did not exhibit significantly altered K_i values. The dramatically impaired binding properties displayed by the W55A/Y195A mutant further supported the importance of these two aromatic residues for MLA binding. This double mutant displayed some specific [^{3}H]MLA binding but not to an extent where displacement experiments could be performed (Table 3). Conservative

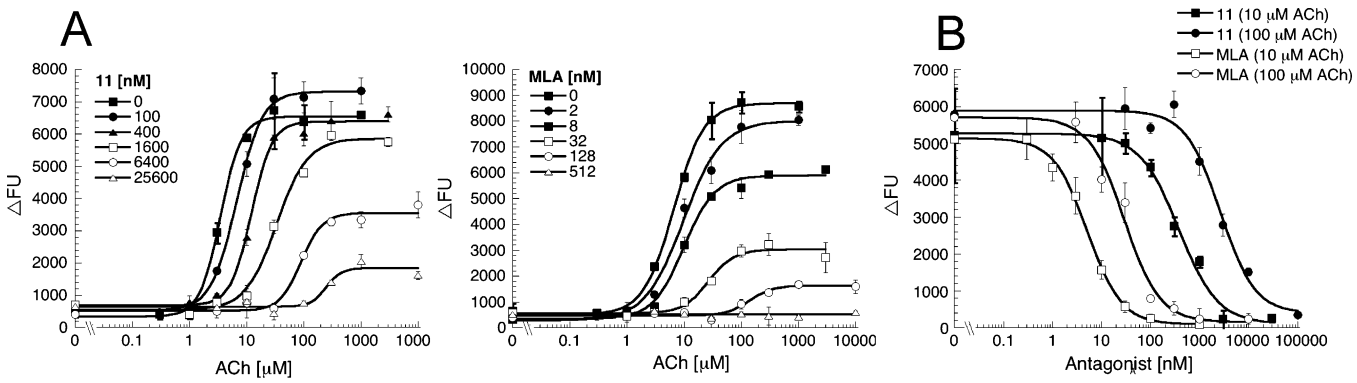

Figure 4. Nature of the antagonism of the caracurine V analogue **11** and MLA at the human α7 nAChR coexpressed with human Ric-3 in tsA-201 cells in the FMP assay: (A) Concentration−response curves for ACh in the absence of or in the presence of five different concentrations of compound **11** or MLA; (B) Concentration−inhibition curves for compound **11** and MLA using two diffent ACh concentrations. The figure depicts data from single representative experiments, and data are given as the mean ± SD of duplicate determinations.

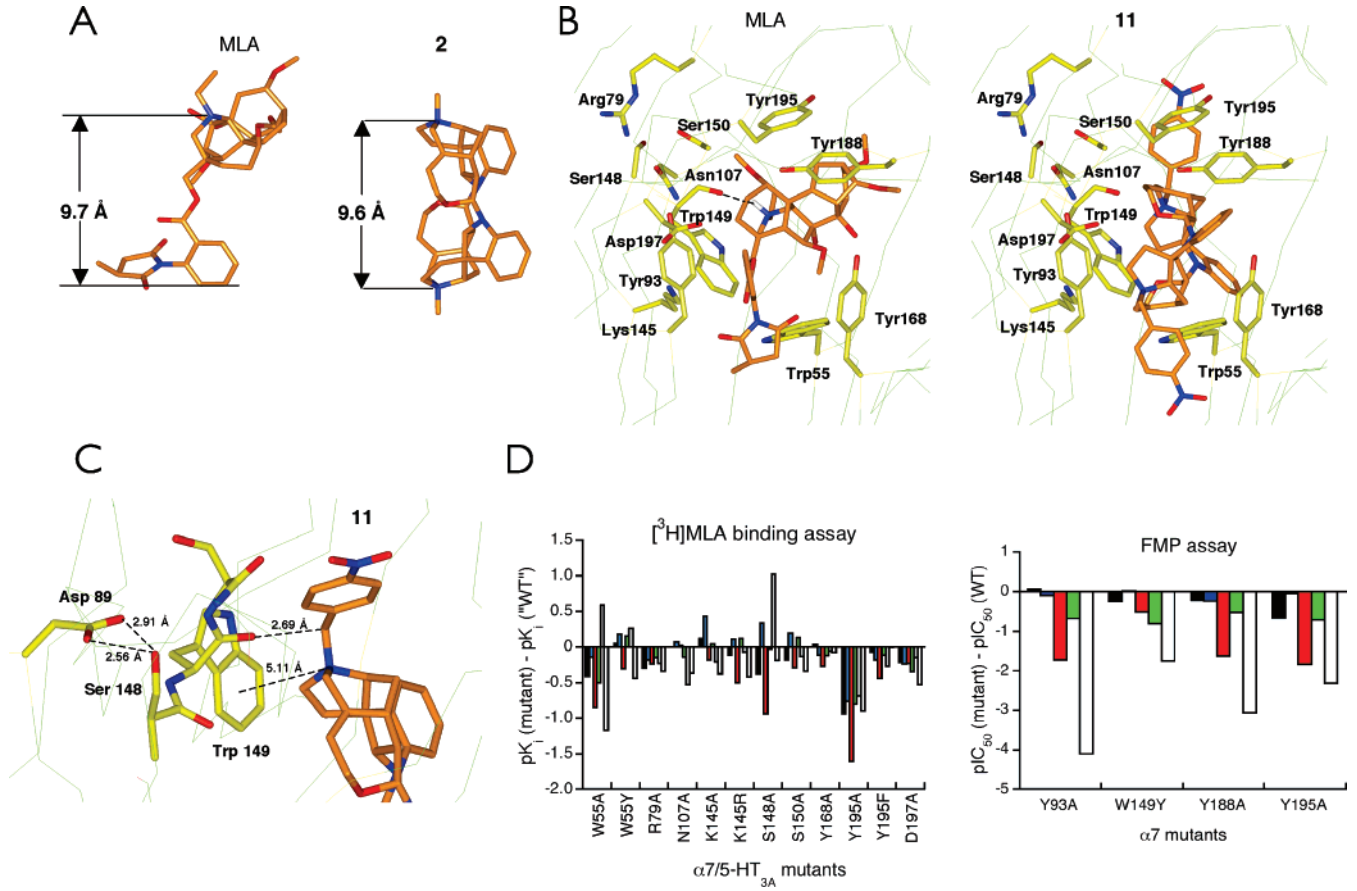

Figure 5. Binding modes of MLA and compound **11** to the α7 nAChR. (A) The 3D structures of MLA and compound **2**. The distances between the cationic nitrogen atom and the distal part of the phenyl ring in MLA and between the two cationic quarternary nitrogen atoms in compound **2** are shown. (B) Homology model of the amino-terminal domain of the α7 nAChR with MLA or compound **11** bound. The residues in α7 subjected to mutagenesis in the present study are indicated. (C) Detail of the homology model of the amino-terminal domain of the α7 nAChR with compound **11** bound. The cation−π and CH−O interactions between compound **11** and the Trp^{149} residue in α7 and the hydrogen bond between the Asp^{89} and Ser^{148} residues in the receptor are indicated. (D) Relative changes in binding affinities (pK_i values) of compounds **2**, **7**, **11**, **14**, and **19** and MLA at mutant α7/5-HT_3 chimeras compared to the "WT" chimera in the [^{3}H]MLA binding assay and the relative changes in functional pIC_{50} values of compounds **2**, **7**, **11**, and **14** and MLA at mutant α7 nAChRs compared to WT in the FMP assay. The data columns for the respective compounds are given in black (**2**), blue (**7**), red (**11**), green (**14**), gray (**19**), and white (MLA).

substitutions of the two residues in the mutants W55Y and Y195F did not result in significantly different binding affinities for any of the six compounds compared to the "WT" chimera (Table 3). Finally, MLA, **2**, **7**, and **14** displayed "WT-like" binding affinities to the S148A mutant, whereas the K_i values of **11** and **19** at the mutant were 9-fold increased and 10-fold decreased, respectively, compared to their affinities to the "WT" chimera.

Introduction of the mutations Y93A, W149A, W149Y, and Y188A in the α7/5-HT_3 chimera completely eliminated [^{3}H]-MLA binding to the receptor (Table 3). Although this could suggest that these residues are important for the binding of MLA to the receptor, the lack of binding could also arise from impaired folding of the protein. Furthermore, the lack of radioligand binding to these mutants made it impossible to evaluate the roles of these residues for the binding of compounds

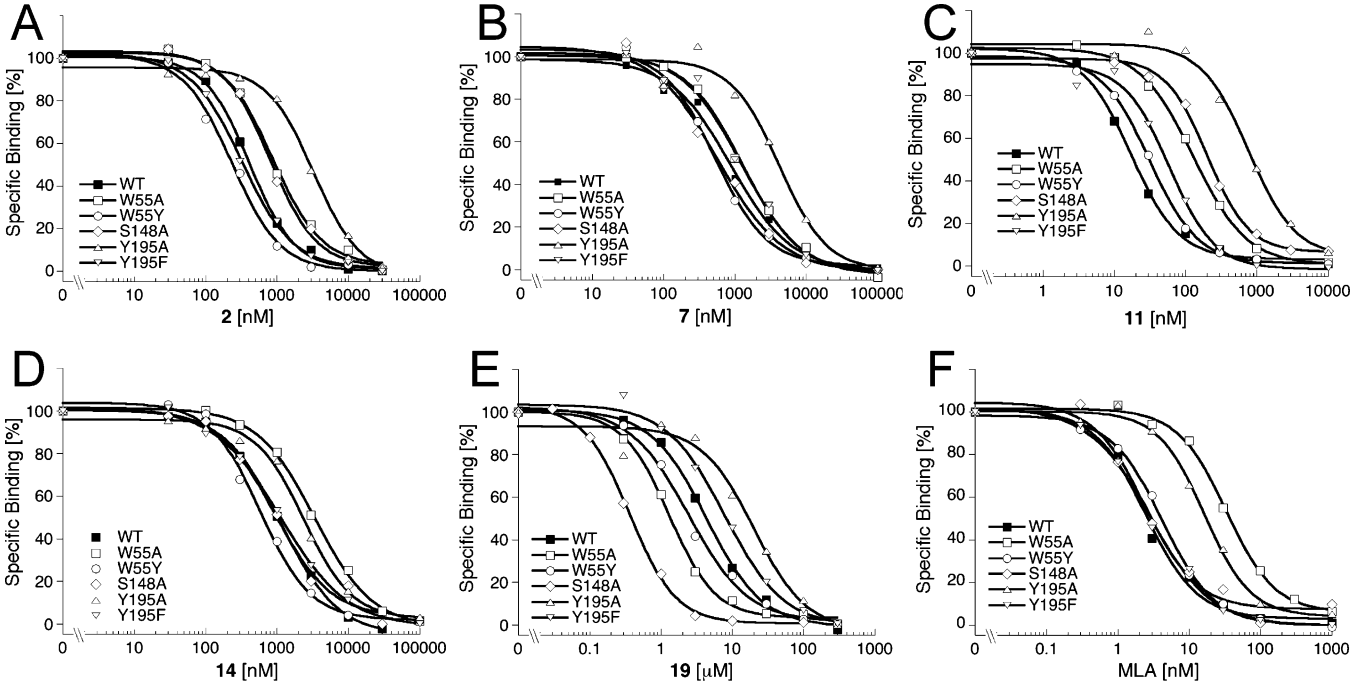

Figure 6. Competition binding of five selected compounds and MLA to "WT" and mutant α7/5-HT_{3A} chimeras: the concentration−inhibition curves of compounds **2** (A), **7** (B), **11** (C), **14** (D), **19** (E), and MLA (F) in the [^{3}H]MLA binding assay. The figure depicts data from single representative experiments, and error bars are omitted for reasons of clarity.

Table 3. Binding Characteristics of Compounds **2**, **7**, **11**, **14**, and **19** and MLA at "WT" and Mutant α7/5-HT_{3A} Chimeras in a [^{3}H]MLA Binding Assay[a]

Receptor	**2**	**7**	**11**	**14**	**19**	MLA
"WT"	330 [6.48 ± 0.02]	840 [6.07 ± 0.01]	18 [7.74 ± 0.01]	970 [6.01 ± 0.01]	4420 [5.35 ± 0.01]	1.6 [8.79 ± 0.02]
W55A	850 [6.07 ± 0.04]	1200 [5.93 ± 0.02]	130 [6.89 ± 0.01]	3100 [5.51 ± 0.02]	1100 [5.94 ± 0.02]	24 [7.62 ± 0.04]
W55Y	300 [6.53 ± 0.02]	560 [6.25 ± 0.03]	37 [7.43 ± 0.04]	690 [6.16 ± 0.03]	2400 [5.61 ± 0.02]	4.5 [8.35 ± 0.06]
R79A	660 [6.18 ± 0.02]	1300 [5.89 ± 0.02]	32 [7.50 ± 0.04]	1400 [5.86 ± 0.04]	7600 [5.12 ± 0.06]	3.5 [8.45 ± 0.04]
Y93A			no significant specific [^{3}H]MLA binding			
N107A	330 [6.48 ± 0.01]	724 [6.14 ± 0.02]	17 [7.76 ± 0.00]	1300 [5.87 ± 0.05]	15000 [4.82 ± 0.02]	3.2 [8.42 ± 0.07]
K145A	250 [6.60 ± 0.01]	320 [6.50 ± 0.02]	28 [7.56 ± 0.03]	890 [6.05 ± 0.04]	7200 [5.14 ± 0.06]	3.9 [8.41 ± 0.07]
K145R	430 [6.37 ± 0.04]	660 [6.18 ± 0.06]	58 [7.24 ± 0.04]	740 [6.13 ± 0.05]	5200 [5.28 ± 0.06]	4.3 [8.37 ± 0.07]
S148A	790 [6.10 ± 0.02]	400 [6.40 ± 0.08]	160 [6.80 ± 0.05]	1000 [5.98 ± 0.04]	430 [6.37 ± 0.06]	2.5 [8.60 ± 0.05]
W149A			no significant specific [^{3}H]MLA binding			
W149Y			no significant specific [^{3}H]MLA binding			
S150A	500 [6.30 ± 0.07]	550 [6.26 ± 0.06]	35 [7.45 ± 0.05]	720 [6.14 ± 0.05]	6000 [5.22 ± 0.05]	3.5 [8.45 ± 0.05]
Y168A	310 [6.51 ± 0.03]	1100 [5.96 ± 0.07]	34 [7.47 ± 0.05]	1300 [5.89 ± 0.04]	5100 [5.29 ± 0.03]	1.9 [8.71 ± 0.07]
Y188A			no significant specific [^{3}H]MLA binding			
Y195A	2900 [5.54 ± 0.01]	4900 [5.31 ± 0.03]	740 [6.13 ± 0.01]	6200 [5.21 ± 0.03]	22000 [4.66 ± 0.05]	13 [7.89 ± 0.02]
Y195F	390 [6.41 ± 0.04]	1300 [5.89 ± 0.04]	50 [7.30 ± 0.05]	1300 [5.90 ± 0.02]	8300 [5.08 ± 0.02]	1.7 [8.78 ± 0.06]
D197A	550 [6.26 ± 0.06]	1500 [5.83 ± 0.02]	31 [7.51 ± 0.10]	2200 [5.66 ± 0.05]	6300 [5.20 ± 0.03]	5.5 [8.26 ± 0.07]
W55A/Y195A			no significant specific [^{3}H]MLA binding			

[a] The K_i values are given in nM (with pK_i ± SEM in brackets). The data are the mean of three to seven individual experiments performed in duplicate as described in Experimental Procedures.

2, **7**, **11**, **14**, and **19**. Thus, we introduced the Y93A, W149A, W149Y, Y188A, and Y195A mutations in the human α7 receptor and characterized the antagonistic properties of the compounds at WT and mutant α7 receptors coexpressed with human Ric-3 in the FMP assay. All of these five mutations had detrimental effects on the potency of ACh, and the mutants also displayed reduced maximal responses to ACh compared to the WT receptor (Table 4 and Figure 7A). The W149A mutant was completely unresponsive to ACh at concentrations up to 30 mM, and the EC_{50} values for ACh at cells expressing the Y93A, W149Y, Y188A, and Y195A α7 mutants were reduced 20-, 375-, 975-, and 65-fold, respectively, compared to the WT receptor (Table 4 and Figure 7A). The antagonistic properties of MLA and compounds **2**, **7**, **11**, and **14** were characterized at WT and mutant α7 receptors using ACh concentrations 2−4-fold higher than the EC_{50} values obtained at the respective receptors. This made it possible to compare the IC_{50} values obtained for the compounds at the respective WT and mutant receptors. The detrimental effects of these mutations on [^{3}H]-MLA binding affinities at the α7/5-HT3A chimera were confirmed in the functional assay, where MLA displayed 2400-, 11-, 217-, and 39-fold higher IC_{50} values at the Y93A, W149Y, Y188A, and Y195A mutants, respectively, than at the WT receptor (Table 4 and Figure 7F). The 4-nitrobenzylcaracurine

Table 4. Functional Characteristics of Compounds **2**, **7**, **11**, **14**, and MLA at WT and Mutant Human α7 nAChRs Coexpressed with Human Ric-3 in tsA−201 Cells in the FMP Assay[a]

Receptor	ACh EC_{50} [$pEC_{50} \pm$ SEM]	IC_{50} [$pIC_{50} \pm$ SEM]				
		2	**7**	**11**	**14**	MLA
WT	4.0 [5.40 ± 0.02]	1.5 [5.82 ± 0.06]	3.0 [5.53 ± 0.02]	0.36 [6.44 ± 0.05]	1.4 [5.86 ± 0.06]	0.0083 [8.08 ± 0.02]
Y93A	81 [4.09 ± 0.02]	1.3 [5.88 ± 0.02]	3.7 [5.43 ± 0.04]	19 [4.71 ± 0.06]	6.6 [5.18 ± 0.05]	10−30 [4.5−5]
W149A	>30.000 [<1.5]	nd	nd	nd	nd	nd
W149Y	1500 [2.80 ± 0.04]	2.7 [5.57 ± 0.04]	2.9 [5.54 ± 0.03]	1.2 [5.93 ± 0.06]	8.9 [5.05 ± 0.02]	0.089 [7.05 ± 0.06]
Y188A	3900 [2.41 ± 0.05]	2.5 [5.61 ± 0.05]	5.3 [5.29 ± 0.05]	15 [4.81 ± 0.08]	4.7 [5.33 ± 0.06]	1.8 [5.74 ± 0.04]
Y195A	260 [3.59 ± 0.05]	7.1 [5.15 ± 0.04]	3.3 [5.48 ± 0.03]	25 [4.60 ± 0.04]	7.1 [5.15 ± 0.06]	0.32 [6.49 ± 0.07]

[a] The EC_{50} values of ACh at the respective receptors are given in μM (with $pEC_{50} \pm$ SEM in brackets), and the IC_{50} values for the antagonists are given in μM (with $pIC_{50} \pm$ SEM in brackets). In the antagonist experiments, ACh concentrations 2- to 4-fold higher than the EC_{50} values obtained for the respective receptors were used: 10 μM ACh for WT, 200 μM ACh for Y93A, 5 mM ACh for W149Y, 10 mM for Y188A and 1 mM for Y195A. Data are the mean of three to five individual experiments performed in duplicate as described in Experimental Procedures. nd: not determined.

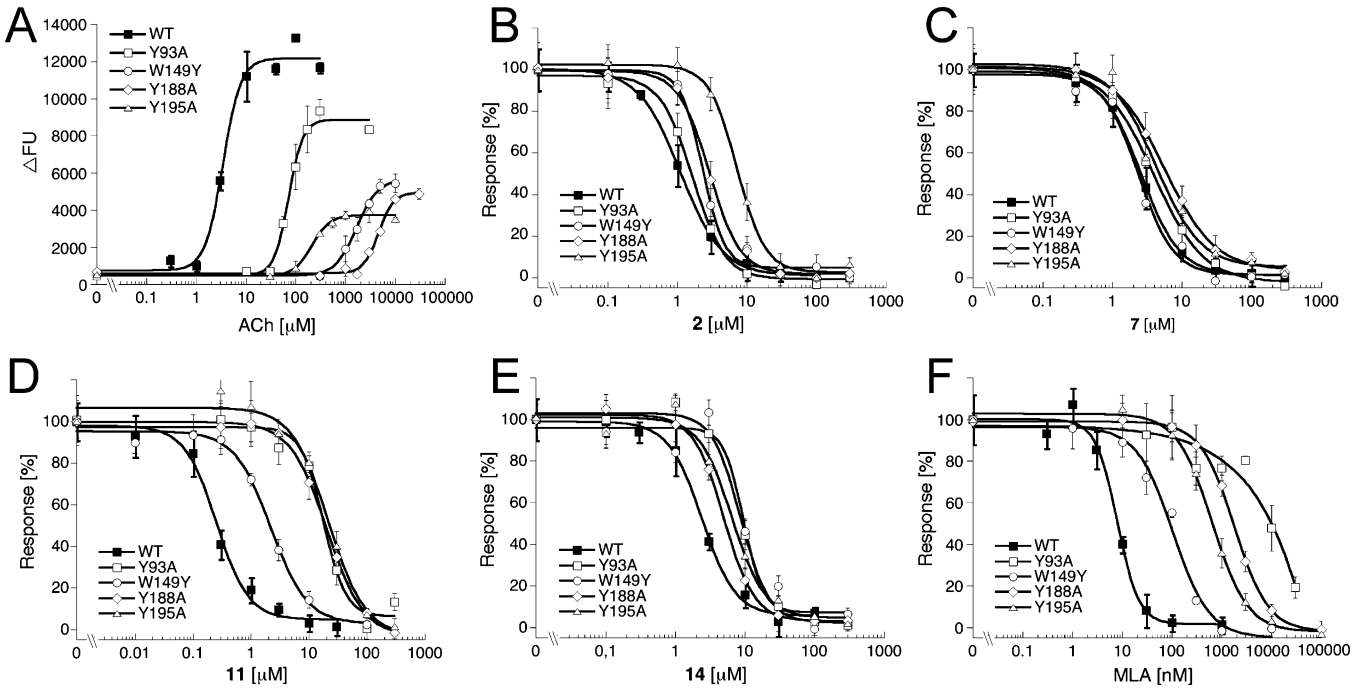

Figure 7. Inhibition of WT and mutant α7 nAChR signaling by four selected compounds and MLA. The concentration−response curves for ACh (A) and the concentration−inhibition curves of compounds **2** (B), **7** (C), **11** (D), **14** (E), and MLA (F) in the FMP assay. The compounds were characterized at WT and mutant α7 nAChRs coexpressed with human Ric-3 in tsA-201 cells in the FMP assay as described in Experimental Procedures using ACh as agonist in assay concentrations of 10 μM, 200 μM, 1 mM, 5 mM, and 10 mM for the WT, Y93A, Y195A, W149Y, and Y188A α7 nAChRs, respectively. The figure depicts data from single representative experiments, and data are given as the mean ± SD of duplicate determinations.

V analogue **11** displayed 53-, 4-, 42-, and 69-fold higher IC_{50} values at the Y93A, W149Y, Y188A, and Y195A mutants, respectively, compared to the WT receptor (Table 4 and Figure 7D). In contrast, the IC_{50} values displayed by analogues **2**, **7**, and **14** compounds at the mutants were either similar or slightly increased compared to those exhibited at the WT receptor (Table 4 and Figures 7B, 7C, and 7E).

Discussion

In the present study, we have investigated the pharmacological properties of a series of bisquaternary caracurine V analogues (**1**−**12**), iso-caracurine V analogues (**13**−**17**), and pyrazino[1,2-*a*;4,5-*a*′]diindole analogues (**18**−**21**) and the two neuromuscular blocking agents alcuronium (**22**) and toxiferine I **(23)** at several LGICs.

Selectivity Profiles of Compounds 1−23. None of compounds **1**−**23** displayed significant activities at the α1 GlyR, at the $GABA_C$ receptor ρ1, or at the α4β2, α3β4, and α4β4 nAChRs, with the exception of a few compounds exhibiting weak activities at α3β4 nAChR (Tables 1 and 2). In contrast, several of the bisquaternary caracurine V and iso-caracurine V analogues displayed binding affinities in the low micromolar to midmicromolar range at the human 5-HT_{3A}R, and the tertiary iso-caracurine V base (**13**) was found to be equipotent as an antagonist at this receptor and at the α7 nAChR. However, most strikingly, the majority of the investigated compounds displayed a significant selectivity for the homomeric α7 nAChR over the other LGICs (Tables 1 and 2). Keeping in mind the previously reported allosteric action of these compounds at mAChRs and their binding affinities at muscle-type nAChRs, the compounds cannot be claimed to be completely selective for the α7 nAChR.[16−18,41,42] Whereas it is quite remarkable that these compounds possess activities at both G-protein-coupled receptors and LGICs for ACh, other α7 nAChR antagonists also display potent antagonism at the muscle-type nAChR, including the prototypic antagonists α-bungarotoxin and (+)-tubocurarine.[1] Interestingly, the binding profiles displayed by the investigated compounds at the M_2 mAChR, the α7 nAChR, and the muscle-type nAChR vary greatly depending on the ring systems and the N-substituents. For example, the *N*-methyl and *N*-allyl substituted muscle relaxants toxiferine I (**22**) and alcuronium (**23**) display 10- to 100-fold higher binding affinities to the

muscle-type nAChR and to the allosteric site of M_2 mAChR than to the α7 nAChR (Table 1).[16,17] In contrast, the dimethyl, monoallyl, and diallylcaracurine V analogues **2**, **3**, and **4**, respectively, display 50- to 100-fold higher binding affinities to the α7 nAChR and to the allosteric site of M_2 mAChR than to the muscle-type nAChR probably because of the totally different 3D structures of the caracurine V and the bisnortoxiferine ring systems.[43] The tertiary caracurine V base (**1**) displays an even higher degree of selectivity between α7 and muscle-type nAChRs, as its low micromolar binding affinities to α7 and the M_2 mAChR is contrasted by it being completely unable to bind to the muscle-type nAChR at concentrations up to 100 μM.[17,42] Finally, the selectivity profile is also determined by the properties of the N-substituents. For example, the *p*-nitrobenzylcaracurine V analogue **11** displays a 10- to 30-fold higher binding affinity at the α7 nAChR than at the muscle-type nAChR and for the allosteric site of M_2 mAChR (Table 1).[16,17]

Structure−Activity Relationship for Compounds 1−23 at the α7 nAChR. The low micromolar binding affinity displayed by caracurine V (**1**) at the α7 nAChR is slightly increased in the bisquaternary dimethyl analogue **2**. As mentioned above, the small difference between the binding affinities displayed by **1** and **2** at this receptor contrasts with the >250-fold higher affinity of the bisquaternary dimethyl analogue **2** at the muscle-type nAChR compared to the tertiary base **1**.[17] This suggests that the binding mode of the caracurine V analogue at the two nAChRs differ somewhat. Whereas introduction of allyl groups at one or both of the two nitrogens in the caracurine V molecule further increases the α7 nAChR affinity (**3** and **4**), analogues with 2-butenyl (**5**), *O*-acetylethanol-2-yl (**6**), cyclohexen-3-yl (**7**), and benzyl (**8**) groups as N-substituents exhibit binding affinities similar to that of the dimethyl analogue **2** (Table 1). Interestingly, the 4-nitrobenzylcaracurine V analogue (**11**) displays a 10-fold higher binding affinity than the benzyl analogue (**8**), whereas a bromo group in the para position of the benzyl group (**10**) does not alter the binding affinity significantly (Table 1). The caracurine V and iso-caracurine V ring systems adopt very similar 3D structures in terms of the relative spatial arrangement of the aromatic rings and the distance between both cationic centers.[43] The most important structural difference is the presence of the allyl alcohol side chain in the iso-caracurine V skeleton that seems to be essential for the high binding for the muscle-type nAChR.[17] Because of similar geometries of both scaffolds, the structure−activity-relationship at α7 nAChR in the iso-caracurine V series is equivalent to that observed for the caracurine V analogues, indicating that the allyl alcohol moiety is not involved in the ligand−α7 nAChR interactions. The binding affinity of the parent compound (**13**) is increased slightly by the introduction of methyl (**14**), cyclohexen-3-yl (**15**), and 2,3-dimethoxybenzyl (**16**) groups as N-substituents, and it is further increased for the 4-nitrobenzyl analogue **17** (Table 1). In the series of pyrazinodiindole analogues (compounds **18**−**21**), the rather poor binding affinities at the α7 nAChR are not affected by the introduction of different N-substituents (Table 1). Since the intercationic distance in the pyrazinodiindole derivative is nearly the same as in the caracurine V scaffold,[18] the most likely explanation for the weak binding affinities of compounds **18**−**21** is a fully flat geometry of the pyrazinodiindole ring system with a totally different relative spatial orientation of the aromatic rings when compared to the caracurine V skeleton.[18] Interestingly, toxiferine I (**22**) and alcuronium (**23**), which have the same intercationic distance as the caracurine V derivatives but a significantly different 3D structure,[43] also exhibit weak binding affinity to the α7 nAChR. The findings indicate that from all investigated ring systems, the caracurine V scaffold has the most favorable geometry for binding to the α7 nAChR. The bisquaternary 4-nitrobenzylcaracurine V analogue **11** exhibited the highest binding affinity in the series (K_i = 29 nM), being only 5 times weaker than the selective α7 nAChR antagonist MLA.

A reasonable correlation exists between the binding affinities of the 23 investigated compounds at the human α7 nAChR and their antagonistic potencies at the receptor in the FMP assay (Figure 3B). In concordance with the rank order obtained in the [^{3}H]MLA binding assay, the monoallyl, diallyl, and 4-nitrobenzylcaracurine V analogues **3**, **4**, and **11**, respectively, are the most potent α7 antagonists in the series, whereas the remaining caracurine V analogues are equipotent displaying low micromolar IC_{50} values (Table 2 and Figure 3A). In contrast to the caracurine V series, the gradual increase in binding affinities observed as a result of the introduction of bulky N-substituents in the iso-caracurine V molecule is not accompanied by concomitant increases in the antagonistic potencies of the compounds (Table 2).

Caracurine V Analogues Are Competitive Antagonists of the α7 nAChR. The antagonism of caracurine V analogue **11** at the α7 nAChR was investigated in greater detail using the FMP assay (Figure 4). The increased EC_{50} values obtained for ACh in the presence of increasing concentrations of **11** (Figure 4A) and the increased IC_{50} value displayed by **11** as the result of an increased ACh concentration (Figure 4B) are both indicative of a competitive antagonist. However, the fact that the maximal response of ACh is decreased with increasing concentrations of **11** suggests a noncompetitive nature of the antagonism exerted by the ligand (Figure 4A). Interestingly, the standard competitive α7 nAChR antagonist MLA displays a very similar antagonist profile (Figure 4). In a recent study of the human α7 nAChR stably expressed in a GH3 cell line, the competitive antagonists MLA and α-bungarotoxin have exhibited noncompetitive antagonist profiles in a fluorescence-based Fluo-4/Ca^{2+} assay, and the inability to distinguish between competitive and noncompetitive antagonists in this assay was attributed to the transient Ca^{2+} kinetics.[44] We will refrain from speculating on the possible reasons for the "mixed" competitive/noncompetitive antagonist profiles of **11** and MLA at the receptor in this study. However, the fact that binding of **11** to the α7 nAChR involves several amino acid residues in the so-called "aromatic box" forming the binding pocket for the positively charged amino group of nAChR agonists and competitive antagonists (Figure 5B) strongly indicates that the caracurine V analogue is a competitive antagonist competing ACh for binding to the α7 nAChR.[2,45,46]

Binding Mode of MLA to the α7 nAChR. In the A-AChBP−MLA crystal structure, MLA displays a key cation−π interaction with Trp^{147} and major interactions with the Tyr^{188}, Tyr^{195}, Tyr^{93}, and Tyr^{55} residues of A-AChBP.[36] Four of these five residues are conserved in the α7 nAChR, whereas Tyr^{55} in A-AChBP corresponds to a Trp residue in the receptor. The binding characteristics displayed by MLA at the Y188A, Y195A, W149A, W149Y, Y93A, W55A, and W55Y α7/5-HT_{3A} mutants (Table 3 and Figure 6F) and the functional properties displayed by the antagonist at Y188A, Y195A, W149Y, and Y93A α7 mutants (Table 4 and Figure 7F) substantiate the key involvement of these corresponding residues in the binding of MLA to the α7 nAChR. Whereas the Tyr^{55} residue in A-AChBP forms a hydrogen bond to the ester carbonyl group in MLA in the

A-AChBP−MLA crystal structure,[36] the corresponding Trp[55] residue in the α7 nAChR is unable to form a direct hydrogen bond to this ester carbonyl group of the ligand. Instead, a hydrogen bond between the residue and MLA may be formed via a water molecule located at a position corresponding to that of the hydroxyl group of Tyr[55] in A-AChBP. All in all, it is reasonable to conclude that MLA binds to the amino-terminal domain of α7 nAChR in the same way as to A-AChBP (Figure 5B). The mutations of the Arg[79], Ser[148], Ser[150], Asn[107], Asp[197], Lys[145], and Tyr[168] residues were introduced in α7 nAChR to investigate the binding modes of the caracurine V, iso-caracurine V, and pyrazino[1,2-*a*;4,5-*a*′]diindole analogues, and in accordance with the considerable distances between these residues and MLA in the homology model of the amino-terminal domain of α7, none of these mutations had any significant effect on the binding properties of MLA (Figure 5B and Table 3).

Binding Mode of Compound 11 and the Other Analogues to the α7 nAChR. In previous studies, the classical nAChR antagonist (+)-tubocurarine and its bisquaternary fully methylated analogue metocurine iodide have been demonstrated to bind in different conformations to the AChBP and the muscle-type nAChR.[47,48] Thus, in order to be able to identify possible differences in the binding modes of the caracurine V, iso-caracurine V, and pyrazino[1,2-*a*;4,5-*a*′]diindole analogues, we included the dimethyl analogue from each of the three series, compounds **2**, **14**, and **19**, in the mutagenesis study. Furthermore, the dihexenyl and bis(4-nitrobenzyl)caracurine V analogues **7** and **11** were included to elucidate the roles of the N-substituents for α7 binding.

Binding of compound **11** and the other caracurine V, iso-caracurine V, and pyrazino[1,2-*a*;4,5-*a*′]diindole analogues to the α7 nAChR is centered in a cation−π interaction between one of the cationic quaternary nitrogen atoms in the ligand and the Trp[149] residue of the receptor (Figures 5B and 5C). Furthermore, the caracurine V analogue also forms a CH−O interaction with the carbonyl group of the Trp[149] residue, similar to what has been observed for carbamoylcholine in its complex with L-AChBP (Figures 5B and 5C).[38] Because of the lack of [^{3}H]MLA binding to W149A α7/5-HT$_{3A}$ and the lack of response to ACh exhibited by W149A α7, the effects of this mutation on the binding of the five selected compounds could not be investigated. However, docking of compound **11** into the α7 homology model strongly suggests that the caracurine V analogue shares the cation−π interaction with Trp[149] with virtually all known orthosteric nAChR ligands.[2,45,46] Furthermore, the fact that the functional IC$_{50}$ values obtained for **2**, **7**, **11**, and **14** at W149Y α7 are similar to or only slightly higher than those displayed at the WT receptor indicates that the presence of an aromatic residue capable of forming cation−π interactions in this position is sufficient to attain proper binding of these ligands (Table 4 and Figure 7).

In addition to the key role of the Trp[149] residue in the α7 nAChR for the binding of the caracurine V analogue **11**, the significant impairment in binding affinities and functional antagonism of the compound at the Y188A, Y93A, W55A, and Y195A mutants is strikingly similar to the pattern observed for MLA (Tables 3 and 4 and Figures 6 and 7). According to the α7 homology model, the Tyr[93] residue forms a weak cation−π interaction with the cationic quarternary nitrogen in compound **11** not engaged in the cation−π binding to Trp[149], whereas the Tyr[188] residue forms a $\pi-\pi$ interaction with one of the benzene rings in **11** (Figure 5B). The impairment of binding to the W55A α7/5-HT$_{3A}$ mutant is proposed to arise from the elimination of a $\pi-\pi$ interaction between the residue and the second benzene ring in **11**, an interaction that is further supported by the recovery of "WT binding affinity" observed for the W55Y α7/5-HT$_{3A}$ mutant (Table 3 and Figure 5B).

One of the N-substituents in compound **11** projects out of this aromatic pocket into a region where it does not appear to form specific interactions with any receptor residues, whereas the other is situated in the vicinity of a couple of receptor residues, including Tyr[195] (Figure 5B). It seems that one of the N-substituents in the caracurine V analogue contributes significantly more to the binding of the ligand than the other, best illustrated by the similar activities displayed by the mono-*N*-allyl and the di-*N*-allyl substituted analogues **3** and **4** at the α7 nAChR (Tables 1 and 2). The spatial orientation of the Tyr[195] residue toward the *p*-nitrobenzyl group of **11** is optimal for a $\pi-\pi$ interaction between the two aromatic rings, and Tyr[195] possibly also forms a hydrogen bond to a nitro-group oxygen atom of **11** (Figure 5B). Introduction of an alanine residue in this position of the receptor results in a significantly decreased binding affinity of **11**, and the partial recovery to "WT binding affinity" observed for **11** at the Y195F mutant substantiates the presence of a $\pi-\pi$ interaction between one of the *p*-nitrobenzyl substituents in **11** and Tyr[195] (Table 3 and Figure 6C). The Y195A mutant also exhibits a reduced binding affinity to the compounds **2**, **7**, **14**, and **19**, a general effect that most likely can be attributed to the flexibility of the C-loop allowing it to fold over the ligand to provide an optimal interaction with the Tyr[195] residue independent of the size of the N-substitutent (Figure 6 and Table 3). Since the nitro group of the *p*-nitrobenzyl group of **11** interacting with Tyr[195] projects further up into the proximity of the Arg[79] residue in the receptor, this positively charged residue could potentially be involved in a electronic interaction with the nitro group of **11**. However, since neither **11** nor the *N*-benzyl-substituted caracurine V analogue **8** displays binding affinities to the R79A α7/5-HT$_{3A}$ mutant significantly different from those displayed at "WT" α7/5-HT$_{3A}$, this does not appear to be the case (Table 3 and data not shown). According to our α7 homology model, the side chain of Arg[79] is highly flexible and could therefore be orientated in another direction than toward the nitro group of **11**.

The S148A α7/5-HT$_{3A}$ mutant exhibits an interesting binding profile because the mutation reduces the binding affinity of **11**, increases the affinity of **19**, and has no significant effect on the binding affinities of compounds **2**, **7**, and **14**. The Ser[148] residue is conserved in all neuronal nAChR subunits, and it forms a strong hydrogen bond to the Asp[89] residue also conserved throughout the LGIC superfamily. In L-AChBP, the corresponding Asp[85] residue has a structural role and may additionally polarize the carbonyl group of Trp[143] in the protein (corresponding to Trp[149] in α7) to provide an increased negative partial charge on the carbonyl oxygen.[38] This negative charge most probably contributes to the compensation of the positive charge of the nitrogen atom in the ligand. Thus, the destruction of the Asp[89]···Ser[148] hydrogen bond brought on by the S148A mutation could lead to a reorientation of the side chain of Asp[89], which in turn could result in a more significant decrease in affinity for high-affinity compounds such as **11** than for low-affinity compound such as **2**, **7**, **14**, and **19** (Figure 5C). It is also expected that the binding affinities of ligands possessing a quarternary nitrogen (such as **11)** and their CH···O electrostatic interaction with the carbonyl group of Trp[149] would be more affected by the S148A mutation than for ligands with a tertiary protonated nitrogen atom (such as MLA), which bind to the receptor via a proper NH···O hydrogen bond (Table 3). The increased binding affinity displayed by compound **19** to the

S148A mutant is somewhat puzzling, however, but it may arise from the pyrazino[1,2-*a*;4,5-*a*′]diindole analogue having a slightly different orientation in the binding pocket compared with the caracurine V analogues due to its different 3D structure, and thus, by chance, it could be easier for binding to the Trp^{149} residue in its new "distorted" orientation in the S148A mutant.

On the basis of the findings discussed above, compound **11** could be docked into our homology model of the amino-terminal domain of the α7 nAChR as shown in Figure 5B. In order to confirm the docking mode of **11** in our α7 model, we subjected the neighboring residues to the aromatic residues forming the binding site of **11** to mutagenesis. Similar to what was observed for MLA binding to α7, introduction of N107A, K145A, K145R, S150A, and D197A mutations in α7/5-HT_{3A} does not alter the binding affinities of any of the five selected analogues significantly (Table 3). In our α7 model with docked compound **11**, none of these residues are situated closely enough to the ligand to form significant interactions with it (Figure 5B). On the other hand, the fact that the Y168A α7/5-HT_{3A} mutant exhibited binding characteristics not significantly different from those of the "WT" chimera was a little surprising considering the proximity of this residue to MLA as well as to compound **11** in the model (Figure 5B). Hence, it remains an open question whether this residue is positioned correctly in our homology model. Another interesting trend in the mutagenesis data is that the degree of impairment in binding affinities and antagonist properties caused by several of the mutations seems to be considerably higher for the high-affinity ligands MLA and **11** than for the low-affinity compounds **2**, **7**, **14**, and **19**, even for residues forming interactions with the "core" of the caracurine V skeleton such as Y93A, Y188A, and W55A (Figure 5D). One possible explanation for this could be that the low-affinity ligands may not be able to properly position themselves for an optimal interaction with these residues and consequently are less affected by changes.

In the present study, several of compounds **1**−**23** have been found to be potent antagonists of the α7 nAChR displaying negligible activities at other neuronal nAChRs and other LGICs. The investigated compounds bind to the orthosteric site of the α7 nAChR interacting with several residues also involved in the binding of agonists and the competitive antagonist MLA to the receptor. Considering that the key residues for the binding of the compounds to the α7 nAChR are conserved in the muscle-type nAChR, it is reasonable to assume that the compounds bind in a similar way to this receptor. In contrast, the inactivity of the compounds at the heteromeric neuronal nAChRs may be attributed to the significantly smaller size of the cavity comprising the orthosteric site observed in homology models of the amino-terminal domains of these nAChRs compared to the cavity in the α7 nAChR model (not shown). In conclusion, the caracurine V and iso-caracurine V analogues join the ranks of other complex natural product compounds such as MLA, (+)-tubocurarine, and several snake and snail peptide toxins as large antagonists able to distinguish between α7 and the other neuronal nAChRs. Although the caracurine V and iso-caracurine V analogues also act as allosteric enhancers of antagonist binding at muscarinic ACh receptors and many of them possess high binding affinities to the muscle-type nAChR, their antagonistic properties at the α7 nAChR make them interesting as pharmacological tools. Furthermore, considering the increasing interest in α7 nAChR ligands as therapeutic agents in recent years, be it agonists, allosteric modulators, or antagonists, it would be interesting to investigate the pharmacophore of caracurine V analogues and related structures further and to explore the in vivo properties of the compounds.

Experimental Procedures

Materials. Culture media, serum, antibiotics, and buffers for cell culture were obtained from Invitrogen (Paisley, U.K.). (*S*)-Nicotine was obtained from Sigma (St. Louis, MO). Quipazine, MLA, and [^{3}H]MLA were obtained from Tocris (Bristol, U.K.), and [^{3}H]-epibatidine and [^{3}H]GR65630 were obtained from Perkin-Elmer (Boston, MA). The cDNAs encoding for the rat α7 nAChR, the human α7 nAChR, and the human Ric-3 were kind gifts from Drs. James W. Patrick (Baylor College of Medicine, Houston, TX), John Lindstrom (University of Pennsylvania Medical School, Philadelphia, PA), and Neil S. Millar (University College London, London, U.K.), respectively. The cDNAs for the mouse 5-HT_{3A}R, the human α1 GlyR, and the human $GABA_C$ ρ1 receptor were obtained from Drs. David J. Julius (University of California, San Francisco, CA), Peter Schofield (Garvan Institute of Medical Research, Sydney, NSW, Australia), and David S. Weiss (University of Alabama, AL), respectively. HEK293 cell lines stably expressing the rat α3β4 nAChR, rat α4β4 nAChR, rat α4β2 nAChR, and the human 5-HT_{3A}R were generous gift from Drs. Ken Kellar and Yingxian Xiao (Georgetown University School of Medicine, Washington, DC), Dr. Joe Henry Steinbach (Washington University School of Medicine, St. Louis, MO), and Dr. Jan Egebjerg (H. Lundbeck A/S, Denmark).[49−51] The generation of the stable HEK293 cell lines expressing the human α1 GlyR and the human $GABA_C$ ρ1 receptor has been described previously.[28,29]

Chemistry. The syntheses of the caracurine V, iso-caracurine V, and 6*H*,13*H*-pyrazino[1,2-*a*;4,5-*a*′]diindole analogues has been described previously.[16−18] The novel compound **21** was obtained

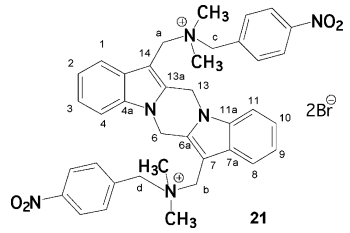

21

from 6,14-bis[dimethyl(aminomethyl)]-6*H*,13*H*-pyrazino[1,2-*a*;4,5-*a*′]diindole[16] and 4-nitrobenzyl bromide according to the general double-quaternization procedure.[17] A solution of 4-nitrobenzyl bromide (115 mg, 0.53 mmol) in $CHCl_3$ (10 mL) was added to a solution of 6,14-bis[dimethyl(aminomethyl)]-6*H*,13*H*-pyrazino[1,2-*a*;4,5-*a*′]diindole[18] (50 mg, 0.13 mmol) in $CHCl_3$ (10 mL). After the mixture was stirred at room temperature for 3 h, the precipitated product was isolated by filtration, washed with $CHCl_3$ (3 × 10 mL), and dried in vacuum at 80 °C. No further purification was necessary as indicated by ^{1}H NMR. Compound **21** (60 mg, 57%) was obtained as a yellow solid: mp >250 °C; IR (ATR) ν (cm^{-1}) 1608, 1522, 1472, 1445, 1346, 1306, 1056, 841; ^{1}H NMR (400 MHz, DMSO-d_6) δ 8.43 (d, J = 8.6 Hz, 4H), 8.05 (d, J = 8.1 Hz, 2H, H-4 and H-11), 7.97−8.02 (m, 6H), 7.42 (m, 2H, H-3 and H-10), 7.34 (m, 2H, H-2 and H-9), 5.90 (br, 4H, CH_2-6, CH_2-13), 5.20 (s, 4H, a-CH_2, b-CH_2), 5.00 (s, 4H, c-CH_2, d-CH_2), 3.11 (s, 12H, 2 × NMe_2^+); ^{13}C NMR (100 MHz, DMSO-d_6) δ 148.6 (2 × C_{ar}−NO_2), 135.7, 135.5, 135.4 (2 × C_{ar}−d-CH_2, C-4a, C-11a) 134.6 (4 × C_{ar}), 128.4 (C-7a, C-14a), 123.9 (C-3, C-10), 123.7, 122.2 (C-3, C-10), 121.4 (C-2, C-9), 119.0 (C-1, C-8), 110.7 (C-4, C-11), 97.5 (C-7, C-14), 63.9 (C-c, C-d), 60.3 (C-a, C-b), 47.8 (2 × NMe_2^+), 38.8 (C-6, C-13); MALDI-MS *m/z* 801.3, 803.3, 805.3 ([M-H]$^+$); Anal. ($C_{38}H_{40}N_6O_4Br_2$) H, N. C: calcd, 56.85; found, 56.40.

Molecular Biology. The human α7 subunit was PCR amplified from its original pMXT vector and subcloned into pCI-neo using *Xho*I and *Xba*I as restriction enzymes. The construction of the α7/5-HT_{3A} chimera consisting of the amino-terminal domain of the rat α7 nAChR and the transmembrane and carboxy-terminal

domains of the mouse 5-HT_{3A} receptor has been described previously.[19] Mutants of the α7/5-HT_{3A} chimera and the human α7 nAChR were constructed using the QuikChange mutagenesis kit according to the manufacturer's instructions (Stratagene, La Jolla, CA). The absence of unwanted mutations was verified by sequencing of the mutant cDNAs.

Cell Culture. The tsA-201 and HEK293 cells lines were maintained at 37 °C in a humidified 5% CO_2 incubator in culture medium [Dulbecco's modified Eagle medium supplemented with penicillin (100 U/mL), streptomycin (100 μg/mL), and 10% fetal bovine serum]. The culture medium used for the stable HEK293 cell lines expressing α4β2, α4β4, and α3β4 nAChRs and 5-HT_{3A}R was supplemented with 1 mg/mL G-418.

[^{3}H]MLA and [^{3}H]GR65630 Binding. [^{3}H]MLA binding experiments with tsA-201 cells transiently transfected with the α7/5-HT_{3A} chimera or with the human α7 nAChR and human Ric-3 were performed as described previously for the chimera.[19] 2×10^6 tsA-201 cells were split, placed into a 10 cm tissue culture plate, and transfected the following day with 8 μg of α7/5-HT_{3A}-pCDNA3.1 or with 4 μg of hα7-pCI-neo and 4 μg of hRic3-pRK5 using Polyfect as a DNA carrier according to the protocol by the manufacturer (Qiagen, Hilden, Germany). The day after the transfection, the culture medium on the cells was changed, and the following day the [^{3}H]MLA binding assay was performed. Briefly, the cells were scraped into 30 mL of assay buffer [50 mM Tris-HCl (pH 7.2)], homogenized using a Polytron for 10 s, and centrifuged for 20 min at 50000*g*. The resulting pellets were homogenized in 30 mL of assay buffer and centrifuged again. Then the cell pellets were resuspended in the assay buffer, and the membranes were incubated with 0.5 nM [^{3}H]MLA and various concentrations of the test compounds. The total reaction volume was 600 μL, and nonspecific binding was determined in reactions with 5 mM (*S*)-nicotine.

The assay mixtures were incubated for 2.5 h at room temperature while shaking. GF/C filters were presoaked for 1 h in a 0.2% polyethyleneimine solution, and binding was terminated by filtration through these filters using a 48-well cell harvester and washing with 3 × 4 mL of ice-cold isotonic NaCl solution. Following this, the filters were dried, an amount of 3 mL of Opti-Fluor (Packard) was added, and the amount of bound radioactivity was determined in a scintillation counter. The fraction of specifically bound radioligand was always <5% of the total amount of radioligand. The binding experiments were performed in duplicate at least three times for each compound.

In the mutagenesis study, 8×10^5 tsA-201 cells were split, placed into a 6 cm tissue culture plate, and transfected the following day with 4 μg of "WT" or mutant α7/5-HT_{3A}-pCDNA3.1 using Polyfect as a DNA carrier according to the protocol by the manufacturer (Qiagen, Hilden, Germany). The [^{3}H]MLA binding assay was performed as described above.

[^{3}H]GR65630 binding to the stable 5-HT_{3A}R-HEK293 cells were performed essentially as for the [^{3}H]MLA binding experiments. The cells were harvested at 80−90% confluency and scraped into the assay buffer [50 mM Tris-HCl (pH 7.2)]. Then the cells were homogenized and centrifuged twice under the same conditions as described above, resuspended in assay buffer, and incubated with 50 pM [^{3}H]GR65630 and various concentrations of the test compounds. The total reaction volume was 600 μL, and nonspecific binding was determined in reactions with 10 μM quipazine. The subsequent incubation, harvesting, and scintillation counting were performed exactly as described for the [^{3}H]MLA binding experiments.

[^{3}H]Epibatidine Binding. The binding experiments with the stable α4β2, α3β4, and α4β4 cell lines were performed essentially as previously described.[19] Briefly, cells were harvested at 80−90% confluency and scraped into assay buffer [140 mM NaCl, 1.5 mM KCl, 2 mM $CaCl_2$, 1 mM Mg_2SO_4, 25 mM HEPES (pH 7.4)], homogenized using a Polytron for 10 s, and centrifuged for 20 min at 50000*g*. Cell pellets were resuspended in fresh assay buffer, homogenized, and centrifuged at 50000*g* for another 20 min. Then the cell pellets were resuspended in the assay buffer, and the cell membranes were incubated with 25 pM [^{3}H]epibatidine in the presence of various concentrations of compounds in a total assay volume of 1500 μL. Nonspecific binding was determined in samples with 5 mM (*S*)-nicotine. The samples were incubated for 4 h at room temperature while shaking. Whatman GF/C filters were presoaked for 1 h in a 0.2% polyethyleneimine solution, and binding was terminated by filtration through these filters using a 48-well cell harvester and washing with 3 × 4 mL of ice-cold isotonic NaCl solution. Following this, the filters were dried, 3 mL of Opti-Fluor (Packard) was added, and the amount of bound radioactivity was determined in a scintillation counter. In both binding assays, the fraction of specifically bound radioligand was always <10% of the total amount of radioligand. The binding experiments were performed in duplicate at least three times for each compound.

FLIPR Membrane Potential (FMP) Assay. The functional characterization of compounds at WT and mutant human α7 receptors coexpressed with human Ric-3 in tsA-201 cells was performed in the FMP assay. 8×10^5 tsA-201 cells were split, placed into a 6 cm tissue culture plate, and transfected the following day with 2 μg of WT or mutant α7-pCI-neo and 2 μg of hRic-3-pRK5 using Polyfect as a DNA carrier according to the protocol by the manufaturer (Qiagen, Hilden, Germany). The day after the transfection, the cells were split and placed into poly-D-lysine-coated black 96-well plates with clear bottoms (BD Biosciences, Bedford, MA). After 16−24 h, the medium was aspirated, and the cells were washed with 100 μL of Krebs buffer [140 mM NaCl, 4.7 mM KCl, 2.5 mM $CaCl_2$, 1.2 mM $MgCl_2$, 11 mM HEPES, 10 mM D-glucose, pH 7.4]. A total of 50 μL of assay buffer (Krebs buffer supplemented with 100 μM genistein) was added to the wells (in the antagonist experiments, various concentrations of the antagonists were dissolved in the buffer), and then an additional 50 μL of assay buffer supplemented with the loading dye was added to each well. Then the plate was incubated at 37 °C in a humidified 5% CO_2 incubator for 30 min and assayed in a NOVOstar plate reader (BMG Labtechnologies, Offenburg, Germany) measuring emission [in fluorescence units (FU)] at 560 nm caused by excitation at 530 nm before and up to 1 min after addition of 33 μL of ACh solution. For the antagonist experiments with the WT α7 receptor, 10 μM ACh was used as the final agonist concentration, and for the mutant α7 receptors ACh concentrations 2- to 4-fold higher than the EC_{50} values for the respective mutant receptors were used. The experiments were performed in duplicate at least three times for each compound.

The functional properties of the compounds at the stable HEK293 cell lines expressing the rat α3β4 nAChR, the human 5-HT_{3A}R, the human α1 GlyR, and the human $GABA_C$ ρ1 receptor were also determined in the FMP assay. The FMP assays were run at these receptors analogously to the α7 nAChR assay except that no genistein was added to the assay buffer. Final agonist concentrations of 20 μM ACh, 1 μM serotonin, 200 μM glycine, and 1 μM GABA were used for the characterization of the test compounds at the α3β4 nAChR, 5-HT_{3A}R, α1 GlyR, and $GABA_C$ ρ1 receptor, respectively.

Data Analysis. Data from the binding experiments were fitted to the equation

$$\% \text{ bound} = \frac{\text{bound}}{1 + ([L]/IC_{50})^n} \times 100$$

and K_i values were determined using the equation

$$K_i = \frac{IC_{50}}{1 + [L]/K_D}$$

where [L] is the radioligand concentration, *n* the Hill coefficient, and K_D the dissociation constant. Since the tracer concentrations of [^{3}H]epibatidine, [^{3}H]MLA, and [^{3}H]GR65630 used in the binding experiments were lower than the K_D values determined for the respective receptors, it was deduced from this equation that the K_i values for the compounds were similar to the obtained IC_{50} values.

Concentration−response curves for agonists and antagonists in the FMP assay were constructed on the basis of the maximal responses at different concentrations of the respective ligands. The curves were generated by nonweighted least-squares fits using the program KaleidaGraph 3.6 (Synergy Software).

Acknowledgment. Drs. Patrick, Lindstrom, Millar, Julius, Schofield, and Weiss are thanked for providing us with various cDNAs, and Drs. Steinbach, Xiao, Kellar, and Egebjerg are thanked for their kind gifts of stable nAChR and 5-HT_{3A}R cell lines. This work was supported by the Lundbeck Foundation and the Danish Medical Research Council.

References

(1) Jensen, A. A.; Frølund, B.; Liljefors, T.; Krogsgaard-Larsen, P. Neuronal nicotinic acetylcholine receptors: structural revelations, target identifications and therapeutic inspirations. *J. Med. Chem.* **2005**, *48*, 4705−4745.

(2) Karlin, A. Emerging structure of the nicotinic acetylcholine receptors. *Nat. Rev. Neurosci.* **2002**, *3*, 102−114.

(3) Reeves, D. C.; Lummis, S. C. The molecular basis of the structure and function of the 5-HT_3 receptor: a model ligand-gated ion channel. *Mol. Membr. Biol.* **2002**, *19*, 11−26.

(4) Lynch, J. W. Molecular structure and function of the glycine receptor chloride channel. *Physiol. Rev.* **2004**, *84*, 1051−1095.

(5) Sieghart, W.; Sperk, G. Subunit composition, distribution and function of $GABA_A$ receptor subtypes. *Curr. Top. Med. Chem.* **2002**, *2*, 795−816.

(6) Corringer, P.-J.; Le, Novère, N.; Changeux, J.-P. Nicotinic receptors at the amino acid level. *Annu. Rev. Pharmacol. Toxicol.* **2000**, *40*, 431−458.

(7) Levin, E. D. *Nicotinic Receptors in the Nervous System*; CRC Press: Boca Raton, FL, 2002.

(8) Arneric, S. P.; Brioni, J. D. *Neuronal Nicotinic Receptors: Pharmacology and Therapeutic Opportunities*; Wiley-Liss, Inc.: New York, 1999.

(9) Paterson, D.; Nordberg, A. Neuronal nicotinic receptors in the human brain. *Prog. Neurobiol.* **2000**, *61*, 75−111.

(10) Cassels, B. K.; Bermudez, I.; Dajas, F.; Abin-Carriquiry, J. A.; Wonnacott, S. From ligand design to therapeutic efficacy: the challenge for nicotinic receptor research. *Drug Discovery Today* **2006**, *10*, 1657−1665.

(11) Romanelli, M. N.; Gualtieri, F. Cholinergic nicotinic receptors: Competitive ligands, allosteric modulators, and their potential applications. *Med. Res. Rev.* **2003**, *23*, 393−426.

(12) Bunnelle, W. H.; Dart, M. J.; Schrimpf, M. R. Design of ligands for the nicotinic acetylcholine receptors: the quest for selectivity. *Curr. Top. Med. Chem.* **2004**, *4*, 299−334.

(13) Young, J. M.; Shytle, R. D.; Sanberg, P. R.; George, T. P. Mecamylamine: new therapeutic uses and toxicity/risk profile. *Clin. Ther.* **2001**, *23*, 532−565.

(14) Shytle, R. D.; Silver, A. A.; Lukas, R. J.; Newman, M. B.; Sheehan, D. V.; Sanberg, P. R. Nicotinic acetylcholine receptors as targets for antidepressants. *Mol. Psychiatry* **2002**, *7*, 525−535.

(15) Nicke, A.; Wonnacott, S.; Lewis, R. J. α-Conotoxins as tools for the elucidation of structure and function of neuronal nicotinic acetylcholine receptor subtypes. *Eur. J. Biochem.* **2004**, *271*, 2305−2319.

(16) Zlotos, D. P.; Buller, S.; Stiefl, N.; Baumann, K.; Mohr, K. Probing the pharmacophore for allosteric ligands of muscarinic M2 receptors: SAR and QSAR studies in a series of bisquaternary salts of caracurine V and related ring systems. *J. Med. Chem.* **2004**, *47*, 3561−3571.

(17) Zlotos, D. P.; Gundisch, D.; Ferraro, S.; Tilotta, M. C.; Stiefl, N.; Baumann, K. Bisquaternary caracurine V and iso-caracurine V salts as ligands for the muscle type of nicotinic acetylcholine receptors: SAR and QSAR studies. *Bioorg. Med. Chem.* **2004**, *12*, 6277−6285.

(18) Zlotos, D. P.; Trankle, C.; Abdelrahman, A.; Gundisch, D.; Radacki, K.; Braunschweig, H.; Mohr, K. 6*H*,13*H*-Pyrazino[1,2-*a*;4,5-*a*′]-diindole analogs: probing the pharmacophore for allosteric ligands of muscarinic M2 receptors. *Bioorg. Med. Chem. Lett.* **2006**, *16*, 1481−1485.

(19) Jensen, A. A.; Mikkelsen, I.; Frølund, B.; Bräuner-Osborne, H.; Falch, E.; Krogsgaard-Larsen, P. Carbamoylcholine homologs: novel and potent agonists at neuronal nicotinic acetylcholine receptors. *Mol. Pharmacol.* **2003**, *64*, 865−875.

(20) Parker, M. J.; Beck, A.; Luetje, C. W. Neuronal nicotinic receptor $\beta 2$ and $\beta 4$ subunits confer large differences in agonist binding affinity. *Mol. Pharmacol.* **1998**, *54*, 1132−1139.

(21) Xiao, Y.; Baydyuk, M.; Wang, H. P.; Davis, H. E.; Kellar, K. J. Pharmacology of the agonist binding sites of rat neuronal nicotinic receptor subtypes expressed in HEK 293 cells. *Bioorg. Med. Chem. Lett.* **2004**, *14*, 1845−1848.

(22) Davies, A. R. L.; Hardick, D. J.; Blagbrough, I. S.; Potter, B. V. L.; Wolstenholme, A. J.; Wonnacott, S. Characterisation of the binding of [^{3}H]methyllycaconitine: a new radioligand for labelling α7-type neuronal nicotinic acetylcholine receptors. *Neuropharmacology* **1999**, *38*, 679−690.

(23) Baker, E. R.; Zwart, R.; Sher, E.; Millar, N. S. Pharmacological properties of the α9α10 nicotinic acetylcholine receptors revealed by heterologous expression of subunit chimeras. *Mol. Pharmacol.* **2004**, *65*, 453−460.

(24) Kurzwelly, D.; Barann, M.; Kostanian, A.; Combrink, S.; Bonisch, H.; Gothert, M.; Bruss, M. Pharmacological and electrophysiological properties of the naturally occurring Pro391Arg variant of the human 5-HT_{3A} receptor. *Pharmacogenetics* **2004**, *14*, 165−172.

(25) Ilegems, E.; Pick, H. M.; Deluz, C.; Kellenberger, S.; Vogel, H. Noninvasive imaging of 5-HT_3 receptor trafficking in live cells: from biosynthesis to endocytosis. *J. Biol. Chem.* **2004**, *279*, 53346−53352.

(26) Krzywkowski, K.; Jensen, A. A.; Connolly, C. N.; Bräuner-Osborne, H. Naturally occuring mutations in the human 5-HT_{3A} gene profoundly impact 5-HT_3 receptor function and expression. *Pharmacogenet. Genomics* **2007**, *17*, 255−266.

(27) Sharif, N. A.; Wong, E. H.; Loury, D. N.; Stefanich, E.; Michel, A. D.; Eglen, R. M.; Whiting, R. L. Characteristics of 5-HT_3 binding sites in NG108-15, NCB-20 neuroblastoma cells and rat cerebral cortex using [^{3}H]-quipazine and [^{3}H]-GR65630 binding. *Br. J. Pharmacol.* **1991**, *102*, 919−925.

(28) Jensen, A. A.; Kristiansen, U. Functional characterisation of the human α1 glycine receptor in a fluorescence-based membrane-potential assay. *Biochem. Pharmacol.* **2004**, *67*, 1789−1799.

(29) Madsen, C.; Jensen, A. A.; Liljefors, T.; Kristiansen, U.; Nielsen, B.; Hansen, C. P.; Larsen, M.; Ebert, B.; Bang-Andersen, B.; Krogsgaard-Larsen, P.; Frølund, B. 5-Substituted imidazol-4-acetic acid analogues: Synthesis, modelling and pharmacological characterization of a series of novel γ-aminobutyric $acid_C$ receptor agonists. *J. Med. Chem.*, in press.

(30) Eiselé, J.-L.; Bertrand, S.; Galzi, J.-L.; Devillers-Thiéry, A.; Changeux, J.-P.; Bertrand, D. Chimaeric nicotinic-serotonergic receptor combines distinct ligand binding and channel specificities. *Nature* **1993**, *366*, 479−483.

(31) Dineley, K. T.; Patrick, J. W. Amino acid determinants of α7 nicotinic acetylcholine receptor surface expression. *J. Biol. Chem.* **2000**, *275*, 13974−13985.

(32) Lansdell, S. J.; Gee, V. J.; Harkness, P. C.; Doward, A. I.; Baker, E. R.; Gibb, A. J.; Millar, N. S. RIC-3 enhances functional expression of multiple nicotinic acetylcholine receptor subtypes in mammalian cells. *Mol. Pharmacol.* **2005**, *68*, 1431−1438.

(33) Williams, M. E.; Burton, B.; Urrutia, A.; Shcherbatko, A.; Chavez-Noriega, L. E.; Cohen, C. J.; Aiyar, J. Ric-3 promotes functional expression of the nicotinic acetylcholine receptor α7 subunit in mammalian cells. *J. Biol. Chem.* **2005**, *280*, 1257−1263.

(34) Cho, C. H.; Song, W.; Leitzell, K.; Teo, E.; Meleth, A. D.; Quick, M. W.; Lester, R. A. Rapid upregulation of α7 nicotinic acetylcholine receptors by tyrosine dephosphorylation. *J. Neurosci.* **2005**, *25*, 3712−3723.

(35) Charpantier, E.; Wiesner, A.; Huh, K. H.; Ogier, R.; Hoda, J. C.; Allaman, G.; Raggenbass, M.; Feuerbach, D.; Bertrand, D.; Fuhrer, C. α7 neuronal nicotinic acetylcholine receptors are negatively regulated by tyrosine phosphorylation and Src-family kinases. *J. Neurosci.* **2005**, *25*, 9836−9849.

(36) Hansen, S. B.; Sulzenbacher, G.; Huxford, T.; Marchot, P.; Taylor, P.; Bourne, Y. Structures of Aplysia AChBP complexes with nicotinic agonists and antagonists reveal distinctive binding interfaces and conformations. *EMBO J.* **2005**, *24*, 3635−3646.

(37) Brejc, K.; van Dijk, W. J.; Klaassen, R. V.; Schuurmans, M.; van Der Oost, J.; Smit, A. B.; Sixma, T. K. Crystal structure of an ACh-binding protein reveals the ligand-binding domain of nicotinic receptors. *Nature* **2001**, *411*, 269−276.

(38) Celie, P. H.; van Rossum-Fikkert, S. E.; van Dijk, W. J.; Brejc, K.; Smit, A. B.; Sixma, T. K. Nicotine and carbamylcholine binding to nicotinic acetylcholine receptors as studied in AChBP crystal structures. *Neuron* **2004**, *41*, 907−917.

(39) Le Novère, N.; Grutter, T.; Changeux, J.-P. Models of the extracellular domain of the nicotinic receptors and of agonist- and Ca^{2+}-binding sites. *Proc. Natl. Acad. Sci. U.S.A.* **2002**, *99*, 3210−3215.

(40) Schapira, M.; Abagyan, R.; Totrov, M. Structural model of nicotinic acetylcholine receptor isotypes bound to acetylcholine and nicotine. *BMC Struct. Biol.* **2002**, *2*, 1.

(41) Buller, S.; Zlotos, D. P.; Mohr, K.; Ellis, J. Allosteric site on muscarinic acetylcholine receptors: a single amino acid in transmembrane region 7 is critical to the subtype selectivities of caracurine V derivatives and alkane-bisammonium ligands. *Mol. Pharmacol.* **2002**, *61*, 160−168.
(42) Zlotos, D. P.; Buller, S.; Trankle, C.; Mohr, K. Bisquaternary caracurine V derivatives as allosteric modulators of ligand binding to M2 acetylcholine receptors. *Bioorg. Med. Chem. Lett.* **2000**, *10*, 2529−2532.
(43) Zlotos, D. P. Stereochemistry of caracurine V, *iso*-caracurine V, bisnortoxiferine, and tetrahydrocaracurine V ring systems. *Eur. J. Org. Chem.* **2004**, *11*, 2375−2380.
(44) Feuerbach, D.; Lingenhohl, K.; Dobbins, P.; Mosbacher, J.; Corbett, N.; Nozulak, J.; Hoyer, D. Coupling of human nicotinic acetylcholine receptors α7 to calcium channels in GH3 cells. *Neuropharmacology* **2005**, *48*, 215−227.
(45) Sine, S. M. The nicotinic receptor ligand binding domain. *J. Neurobiol.* **2002**, *53*, 431−446.
(46) Lester, H. A.; Dibas, M. I.; Dahan, D. S.; Leite, J. F.; Dougherty, D. A. Cys-loop receptors: new twists and turns. *Trends Neurosci.* **2004**, *27*, 329−336.
(47) Gao, F.; Bern, N.; Little, A.; Wang, H. L.; Hansen, S. B.; Talley, T. T.; Taylor, P.; Sine, S. M. Curariform antagonists bind in different orientations to acetylcholine-binding protein. *J. Biol. Chem.* **2003**, *278*, 23020−23026.
(48) Wang, H. L.; Gao, F.; Bren, N.; Sine, S. M. Curariform antagonists bind in different orientations to the nicotinic receptor ligand binding domain. *J. Biol. Chem.* **2003**, *278*, 32284−32291.
(49) Xiao, Y.; Meyer, E. L.; Thompson, J. M.; Surin, A.; Wroblewski, J.; Kellar, K. J. Rat α3/β4 subtype of neuronal nicotinic acetylcholine receptor stably expressed in a transfected cell line: pharmacology of ligand binding and function. *Mol. Pharmacol.* **1998**, *54*, 322−333.
(50) Fitch, R. W.; Xiao, Y.; Kellar, K. J.; Daly, J. W. Membrane potential fluorescence: a rapid and highly sensitive assay for nicotinic receptor channel function. *Proc. Natl. Acad. Sci. U.S.A.* **2003**, *100*, 4909−4914.
(51) Sabey, K.; Paradiso, K.; Zhang, J.; Steinbach, J. H. Ligand binding and activation of rat nicotinic α4β2 receptors stably expressed in HEK293 cells. *Mol. Pharmacol.* **1999**, *55*, 58−66.

JM070574F